Government of Saskatchewan
Ministry of Agriculture

ADF Project Final Report Format

1. **Project title and ADF file number.**
   Project Title: "Establishing transgene-free CRISPR/Cas9 based genome editing platform to improve canola resistance against clubroot disease"
   Project No. ADF20180243

2. **Name of the Principal Investigator and contact information.**

   Dr. Xiao Wei
   Professor
   Organization: Department of Microbiology and Immunology, University of Saskatchewan
   Address: Saskatoon, SK, S7N 5E5;
   Phone: (306) 966-4308;
   E-mail: wei.xiao@usask.ca

3. **Name of the collaborators and contact information.**

   Dr. Gary Peng
   Organization: Agriculture and AgriFood Canada
   Address: 107 Science Place, Saskatoon, SK, S7N 0X2;
   Phone: (306) 385-9410;
   Email: gary.peng@agr.gc.ca

   Dr. Lipu Wang
   Organization: Department of Plant Sciences, University of Saskatchewan
   Address: 51 Campus Drive, Saskatoon, SK, S7N 5A8;
   Phone: (306) 966-8586;
   E-mail: liw791@mail.usask.ca

   Dr. Yangdou Wei
   Organization: Department of Biology, University of Saskatchewan
   Address: 112 Science Place, Saskatoon, SK, S7N 5E2;
   Phone: (306) 966-4447;
   E-mail: yangdou.wei@usask.ca

   Dr. Randy Kutcher
   Organization: Department of Plant Sciences, University of Saskatchewan
   Address: 51 Campus Drive, Saskatoon, SK, S7N 5A8;
   Phone: (306) 966-4951;
   E-mail: randy.kutcher@usask.ca

   Dr. Yu Chen
   Organization: Cargill Canada
   Address: 701 Central Avenue, Aberdeen, SK, S0K 0A0;
   Phone: (306) 253-3455
   E-mail: yu_chen1@cargill.com

4. **Abstract/ Summary**: *An outline on overall project objectives, methods, key findings and conclusions for use in publications and in the Ministry database (**Maximum of 500 words** or one* page).

   Abstract Content: The abstract addresses the following (usually 1–2 sentences per topic):
   - Key aspects of the literature review
   - Problem under investigation or research question(s)
   - Clearly stated hypothesis or hypotheses

- *Methods used (including brief descriptions of the study design, sample, and sample size)*
- *Study results*
- *Conclusions*

The canola (*Brassica napus* L.) crop is continually threatened by the clubroot disease, which significantly affects canola seed quality by reducing oil content and seed weight. Growing clubroot-resistant (CR) cultivars in appropriate rotations remains the most effective solution to control this disease. However, currently available CR varieties carry a single, race-specific, dominant *R* gene, which cannot provide durable resistance and are easily broken down with a shift in the pathogen population. A new alternative strategy based on susceptibility (*S*) genes has been proposed as they have the potential to be durable in the field. Different from conventional breeding, disease resistance can be easily conferred by introducing site-specific mutations to disrupt *S* genes via a precise CRISPR/Cas9 based genome editing tool.

In this project, we developed an *S* gene strategy to improve canola clubroot resistance: First, novel *S* candidate genes were identified from model plant *Arabidopsis thalianna* and their roles in clubroot susceptibility investigated. Then function-confirmed *S* genes were used to search for their corresponding orthologous genes in *B. napus*. Third, the CRISPR/Cas9 sgRNA construct was designed to target these *S* genes and transformed into canola plants using in-house built *Agrobacterium*-mediated canola transformation platform. In the end, identified gene-editing mutant plants were assessed with clubroot disease assays to confirm their conferred clubroot resistance.

The first two *S* genes identified are *ubiquitin conjugating enzyme 13* (*UBC13*) . Inactivation of Arabidopsis *UBC13* genes resulted in enhanced resistance to several pathotypes of the clubroot pathogen, making *UBC13* genes ideal targets for gene editing. Metabolic and transcriptional analysis reaveled that UBC13 contributes to clubroot susceptilibyt by affecting the auxin signaling pathway. In *B. napus*, twelve *UBC13* genes were identified and functionally characterized. Four sgRNA constructs were designed to cover all *BnUBC13* genes and transformed into *B. napus* doubled haploid line DH12075. In total, 78 regenerated plants were obtained for the first sgRNA construct that simultaneously targets five *BnUBC13* genes. In/Del mutations were identified by PCR amplification and DNA sequencing in these lines. Clubroot disease assessment showed that several lines significantly reduced disease severity compared to control plants.

In addition, two well-known gene groups belonging to sucrose transporter genes, *SWEET11* and *12*, were also targeted for gene editing in this project. Two sgRNA target sequences were designed, cloned into one CRISPR/Cas9 vector and transformed into plants. In total, 55 and 70 regenerated plants were obtained for *SWEET11* and *SWEET12*, respectively, among which several lines displayed reduced disease severity to the clubroot infection.

In summary, this project successfully established an in-house CRISPR/Cas9 based genome editing platform that facilitates gene functional study and trait characterization in *B. napus*. An *S* gene based strategy to improve clubroot resistance has been developed and demonstrated in concept through this project. This study will expedite the breeding process and, consequently, reduce the investment costs to the canola industry in the breeding of new cultivars. Eventually, the knowledge, germplasm, molecular markers and CRISPR/Cas9 genome editing tools generated from this project will accelerate breeding cycles and benefit the Canadian canola industry.

5. **Extension Messages:** *key outcomes and their importance for producers/processors and the relevant industry sector (**3-5 bullet points** **in lay language).***

- An in-house CRISPR/Cas9 based genome editing platform is available to accelerate gene discovery, functional characterization and agronomy trait improvement in *B. napus*.
- An *S* gene based gene editing strategy to improve clubroot resistance is developed and available to identify and characterize alleles that confer durable race-independent resistance against clubroot.
- Two novel *S* genes were identified and functionally characterized in Arabidopsis.
- CRISPR/Cas9 edited mutant alleles in 22 *B. napus S* genes will be available to improve clubroot resistance by either providing molecular markers or resistant germplasms.

6. **Introduction:** *Brief project background and rationale (**Maximum of 1500 words or 1.5-3 pages**).*

Canola industry contributes $26.7 billion to the Canadian economy each year (Canola Council of Canada, 2017). However, annual loss due to abiotic stress and disease is in tens of millions of dollars. One of the major canola diseases is clubroot, which caused canola yield loss of up to 50% in severely infected fields in Alberta and significantly affects canola seed quality by reducing oil content and seed weight.

Clubroot disease continues its spread in western Canada, including all three prairie provinces. Growing clubroot-resistant cultivars in appropriate rotations remain the most effective solution for the long-term management of this disease. However, current clubroot resistance largely relies on race-specific, single, dominant *R* genes, which are easily broken down with a shift in the pathogen population (Rahman *et al.*, 2014). In Canada, most canola cultivars are susceptible and current resistant cultivars have showed substantial resistance erosion in many Alberta fields. Novel sources with new resistance genes introgressed into elite canola germplasm will help improve the diversity and durability of clubroot resistance. Conventional breeding strategy is time consuming, labor intensive and requires multiple rounds of crossing and selection to generate improved genetic resources, which typically takes 5-7 years to complete. Additionally, clubroot resistance sources are very limited, despite extensive search and screening. This cannot keep pace with the need to fight this rapidly evolving pathogen.

In recent years, targeted genome editing technologies have emerged that show great promise for crop improvement. One of these revolutionary technologies is the Clustered Regularly Interspaced Short Palindromic Repeat (CRISPR)/CRISPR-associated protein 9 (CRISPR/Cas9) system, which relies on an endonuclease, the Cas9 protein to induce a DNA double-strand break (DSB) at the target genome site directed by an engineered sequence-specific single guide RNA (sgRNA). It then stimulates non homologous end joining (NHEJ) or homology-directed repair (HDR) to generate new DNA variants in the genome (Sander and Joung, 2014). Therefore, this technology has the potential to accelerate plant breeding and is analogous to "molecular scissors" capable of converting inferior genes into desirable genes in existing elite germplasm, which would be valuable for breeders to expedite the breeding cycles.

In addition, genome editing of elite varieties does not introduce potentially deleterious alleles, as occurs during crossing and recombination, or requires time-consuming repeated backcrosses to reconstruct the elite genetic background. The most important advantage of CRISPR/Cas9 is its multiplexing capability, which can simultaneously edit multiple targets in a single generation (Scheben *et al.*, 2017). This allows rapid trait stacking and editing of gene networks or redundant pathways in their native context to improve quantitative traits. Multiplexing is particularly useful in polyploid crops such as canola, which has two sets of chromosomes and multiple-copy genes. Meanwhile, the latest version of CRISPR/Cas9 allows genome editing without introducing foreign transgenes (Yin *et al.*, 2017). This can reduce potential risks and regulatory requirements that may apply to transgenic crops. With its simplicity, high efficiency and low cost, CRISPR/Cas9-based tools have been rapidly applied into major crop species, including maize, rice and wheat.

In this proposed project, we aim to establish a CRISPR/Cas9-based genome-editing platform to support canola breeding programs against clubroot disease. This platform can be integrated into the current breeding strategy to accelerate breeding cycles. In the pre-breeding stage, the genome-editing platform can validate functions of candidate resistance genes in a rapid, effective and inexpensive fashion. The Information and knowledge of novel resistance genes will be transferred to breeders and industry. In the breeding stage, this platform can precisely and efficiently create desirable allelic variant in elite germplasms to improve clubroot resistance.

7. Objectives and the progress towards meeting each objective.

Objectives **(Please list the original objectives and/or revised objectives if Ministry-approved revisions have been made to original objectives. A justification is needed for any deviation from original objectives).**	**Status** **(e.g. completed/not completed)**
a) Establish transgene-free CRISPR/Cas9 based genome editing platform to support canola breeding programs	Completed
b) Identify novel clubroot resistance genes and create novel resistance allelic variants in elite canola germplasms	Completed

Please add additional lines as required.

8. **Methodology:** *Specify project activities undertaken during the entire project period (without referring to previous progress report). Include approaches, experimental design, methodology, materials, sites, etc.* ***(Maximum of 5 pages)***

Objective 1:

Construction of the CRISPR/Cas9 vector

Sequence-specific single-guide RNAs (sgRNAs) were designed using the web-based tool CRISPR-P (http://cbi.hzau.edu.cn/cgi-bin/CRISPR). The target sites were selected for the target gene based on their location in the gene, GC% content and putative off targets. The binary pYLCRIPSR/Cas9 multiplex genome targeting vector system was provided by Prof. Yaoguang Liu (South China Agriculture University, China). It includes pYLCRISPR/Cas9Pubi-H and pYLCRISPR/Cas9P35S-B, in which Cas9 is driven by the maize ubiquitin promoter (Pubi) and the cauliflower mosaic virus 35S promoter (P35S), respectively. The system also contains four plasmids with sgRNA cassettes driven by promoters of AtU3b, AtU3d, AtU6-1 and AtU6-29. This system was used for construct assembly according to a method previously described by (Ma *et al.*, 2015).

Plant materials and Agrobacterium-mediated transformation

The *Brassica napus* doubled haploid line DH12075 (provided by Dr. Fengqun Yu, AAFC, Saskatoon Research and Development Center) was used as the transformation recipient in this study. The *Agrobacterium tumefaciens*-mediated hypocotyl transformation followed the protocol outlined by (Zhou *et al.*, 2002) (Figure 1.1). **1)** Seed germination. The seeds were cleaned three times with sterilized water and then sterilized with 70% ethanol for 1 min, followed by 20% of bleach disinfectant (the active ingredient is approximately 1.0% NaClO in the ratio of mass-to-volume) for 10 min. Then seeds were rinsed 4 times with sterilized water before being transferred to a 1/2 MS medium. Seeds were kept in complete dark for 7 days. **2)** Agrobacterium preparation. Agrobacterium strain GV3101 harbouring the expression vector was revived from −80 ℃ stock for approximately 30 min (28 ℃, 180 rpm). Then, 50 µL of the revived Agrobacterium was inoculated into 20 mL LB liquid medium and cultured at 28 ℃ (180 rpm) for approximately 12 h. When OD600 reached approximately 0.4, 2 mL of culture was taken for centrifugation (3 min, 6000 rpm) to collect the pellet. The supernatant was removed and the pellet rinsed twice with liquid infection medium (LIM, 4.4 g/L MS, 30 g/L sucrose, pH=5.84-5.88, 200 µM acetosyringone). The resuspended pellet was kept at 4 ℃ for further infection. **3)** Agrobacterium infection and cocultivation. Hypocotyls were cut to approximately 1 cm into a sterilized plate containing 18 mL pre-added LIM, and then the aforementioned 2 mL of the resuspended pellet was added to the plate and allowed to infect for approximately 10 min. Next, the infected hypocotyls were placed in the cocultivation medium (4.4 g/L MS, 30 g/L sucrose, 18 g/L mannitol, pH=5.84-5.88, 1 mg/L 2,4-D, 0.3 mg/L kinetin, 200 mM acetosyringone and 8 g/L agar) for two days in the dark, at 25 °C. **4)** Calli induction. All the hypocotyls were transferred to calli-inducing medium (CIM, 4.4 g/L MS, 30 g/L sucrose, 18 g/L mannitol, pH=5.84-5.88, 1 mg/L 2,4-D, 0.3 mg/L kinetin, STS (0.1 M $Na_2S_2O_3$: 0.1 M $AgNO_3$ = 4:1), 300 mg/L timentin, 25 mg/L hygromycin and 8 g/L agar) for 20 days at 2000–2500 lux. **5)** Shoots induction. all the hypocotyls with embryogenic calli were transferred into a shoot-inducing medium (SIM, 4.4 g/LMS, 10 g/L glucose, 0.25 g/L xylose, 0.6 mg/L MES, pH=5.84-5.88, 2.0 mg/L zeatin, 0.1 mg/L IAA, 3 mg/L $AgNO_3$, 300 mg/L timentin, 25 mg/L hygromycin and 8 g/L agar) for shoots regeneration, and renewed the medium every 2–3 weeks until at least 3 leaves appeared. **6)** Roots induction and plantlet regeneration. The induced shoots were transferred into root-inducing medium (RIM, 4.4 g/L MS, 10 g/L sucrose, 300 mg/L timentin and 8 g/L agar, pH=5.84-5.88). When plantlets grew roots and 4-6 leaves, they were transplanted into pots with nutritive soil and cultivated in a greenhouse.

Identification of mutant transgenic plants

polymerase chain reaction (PCR) was performed to amplify the genomic region surrounding the CRISPR target sites using specific primers. The PCR products were directly sequenced to identify the mutations. The sequences were compared to WT sequences to detect the presence of indels. The sequencing chromatograms were also examined

to identify overlapping traces in the region surrounding the protospacer adjacent motif (PAM), which are indicative of the presence of mutations.

Objective 2:

Arabidopsis lines and *Plasmodiophora brassicae* pathotype

Three Arabidopsis lines, wild type Columbia (Col-0), double mutant *ubc13* and *AtUbc13A*-transformed *ubc13* (AtUbc13A/*ubc13*) (the latter two lines were created in our lab). *P. brassicae* pathotypes 3H, 5X-LG2 and 3A were used in this study.

Seeding and growing conditions

Seeds were grown in Sunshine #3 soil (SunGro Horticulture, Vancouver, BC) in 4-inch wide by 4-inch tall pots, with three pots for each line and pathotype, three biological repeats were performed for this experiment. The plants were grown in a growth chamber at 22/16 °C (day/night) with a 16 h photoperiod until sample collection. Plants were watered daily, from the bottom up allowing water to soak in from the bottom of the pots.

Preparation and inoculation of *P. brassicae* pathotypes

Resting spore suspension of *P. brassicae* 3H, 5X-LG2 and 3A were prepared from galled roots of *B. napus* L. that were previously frozen at -20 °C. The galled roots were homogenized in a blender with distilled water, then plant materials were removed from the suspension by filtering the homogenate through eight layers of cheesecloth. The resting spore concentration was measured by haemocytometer and then diluted to a final concentration of 1 x 10^8 spores/mL. For seedling inoculation, each 7-day-old seedling was inoculated with 3 mL of 1 x 10^7 spores/mL of resting spore inoculum. For soil inoculation 20 mL of 1 x 10^7 spores/mL resting spore inoculum were inoculated onto the surface of the soil where seeds were planted.

Clubroot severity assessment

Four weeks after inoculation, the plants were removed from the soil and gently washed with water to prevent breakage of roots for proper disease rating. The roots were examined and photographed for galls, and the severity of infection was evaluated using a 0 to 5 scale as described previously with minor modifications (Hatakeyama *et al.*, 2013): 0, no visible symptoms; 1, very small galls mainly on lateral roots and that do not impair the main root; 2, small galls covering the main root and few lateral roots; 3, medium to large galls, also including the main root; and 4, severe galls on lateral root, main root or rosette; fine roots completely destroyed; and 5, big club on main root and hypocotyl, leading degradation of root; plant growth is affected severely and plants is dying. The disease severity index of each line was calculated following Hatakeyama *et al*. (2013).

Metabolite profiling

Metabolite profiling was performed in The Metabolomics Innovation Centre, University of Aberta, Canada. WT and *ubc13* plants were inoculated with *P. brassicae* pathotype 3H or water. Two weeks after inoculation plant roots were collected, washed with distilled water, and immediately frozen in liquid nitrogen. Around 20 plants per genotype were pooled together as one biological replicate, including three replicates for each treatment. Approximately 80 mg per ground frozen sample was extracted and labelled with ^{12}C-/^{13}C-isotope according to a previously reported protocol (Guo and Li, 2009). The $^{12}C_2$-labeled individual sample was mixed with $^{13}C_2$-labeled reference sample in equal volume. The mixture was ready to be analyzed by LC-MS. Prior to LC-MS analysis of the entire sample set, quality control (QC) sample was prepared by equal volume mix of a ^{12}C-labeled and a ^{13}C-labeled pooled sample.

The sample extracts were analyzed using an Agilent 1290 liquid chromatograph (LC) linked to Agilent 6546 QTOF mass spectrometer (MS). The analytical conditions were as follows, HPLC column: Agilent eclipse plus reversed-phase C18 column (150 x 2.1 mm, 1.8 µm particle size); the mobile phase consisted of solvent A, pure water with 0.1% formic acid, and solvent B, acetonitrile with 0.1% formic acid. Sample measurements were performed with a gradient program: t = 0 min, 25% B; t = 10 min, 99% B; t = 15 min, 99% B; t = 15.1 min, 25% B; t=18 min, 25% B. The flow rate is 400 µL/min. The column oven was set to 40°C.

A total of 30 LC-MS data from 2-channel analysis (15 LC-MS data, including 3 QC in each channel) were first exported to .csv file with Agilent MassHunter software. The exported data were uploaded to IsoMS Pro 1.2.15. After data quality check, data processing was performed. Peak pairs without data present in at least 80.0% of samples in any group were filtered out. Data were normalized by Ratio of Total Useful Signal.

Analysis was performed using IsoMS Pro 1.2.15 (NovaMT Inc.) and NovaMT Metabolite Database v2.7. Three-tier ID approach was used to perform metabolite identification. In tier 1, peak pairs were searched against a labeled metabolite library (CIL Library) based on accurate mass and retention time. The CIL Library contains more than 1,500 experimental entries. In tier 2, linked identity library (LI Library) was used for the identification of remaining peak pairs. LI Library includes over 9,000 pathway-related metabolites, providing high-confidence putative identification results based on accurate mass and predicted retention time matches. In tier 3, the remaining peak pairs were searched, based on accurate mass match, against the MyCompoundID (MCID) library composed of 8,021 known human endogenous metabolites (zero-reaction library), their predicted metabolic products from one metabolic reaction (375,809 compounds) (one-reaction library) and two metabolic reactions (10,583,901 compounds) (two-reaction library).

Metabolites that were identified in tier 1 and tier 2 as high-confidence results were used for pathway analysis. The pathway analysis was performed using Global Test as enrichment analysis and Relative-betweeness Centrality as topology analysis in MetaboAnalyst (www.metaboanalyst.ca).

RNA extraction and qRT-PCR

RNA extraction was performed according to the protocol from Qiagen RNeasy Plant Mini Extraction Kit. Three samples for each control and inoculated were extracted. cDNA synthesis was done following the protocol using Qiagen QuantiTect Reverse Transcription Kit. The primers used for qRT-PCR were listed below. Each sample was done for 3 technical replicates. qRT-PCR was performed according to the protocol using Qiagen QuantiTect SYBR Green PCR Kit. A total of 20 µL/well was loaded onto a 96-well plate, which was placed into the Applied Biosystems thermocycler following cycling conditions from the protocol, yielding Ct (threshold) values for each samples. ΔCt was calculated from the Ct value of a sample – Ct mean of *ACTIN2* (housekeeping reference gene). ΔΔCt was calculated from ΔCt Inoculated - ΔCt Control for relative quantification. 2^(-ΔΔCt) was then calculated for 3 technical replicates and averaged, resulting in a relative gene expression for each sample.

Locus	Gene Name	Sequence (5' - 3')	Function description
AT3G23050	IAA7/ AXR2	F:TCGGCCAACTTATGAACCTC R:CTTCTCCTTGGGAACAGCAG	Auxin induced gene, repressor of auxin-inducible gene expression
AT1G04250	IAA17/ AXR3	F:TCTTCCCGGTGGAGATACAG R:TTGATTTTTGGCAGGAAACC	Auxin induced gene, repressor of auxin-inducible gene expression
AT4G32280	IAA29	F:TGAAGATTGCGACAGAGAAG R:GAACAGATTCCGCAAAGATC	Auxin induced gene, involved in IAA signaling. Downstream target of PIF4
AT4G03400	DFL2	F:AACCCGTCTCTTGCTTCTCA R:CAACGTTCACACCAATCCAG	Encode GH3-related gene in red light-specific hypocotyl elongation
AT3G62980	TIR1	F:AGATAAGGGACTGCCCGTTT R:GACCAGCCACTGTTCGGTAT	Encode TIR-like auxin receptor
AT1G73590	PIN1	F:GGCAGCTTTGCCGCAAG R:TCATAGACCCAAGAGATTG	Encode auxin efflux carrier in shoot and root development
AT5G57090	PIN2	F:TGGTATTCGAGGTGATCTC R:GTAGTAGAGTACTGTTACAG	Encode auxin efflux carrier shoot and root development

Bioinformatics analyses

The genome structure and location of *BnUBC13* genes were retrieved from Ensemble Plants (https://plants.ensembl.org/index.html), illustrating the annotated protein-coding regions. The protein domain was

found in the NCBI Conserved Domain Search (https://www.ncbi.nlm.nih.gov/Structure/cdd/wrpsb.cgi), while the subcellular location was predicted by UniProt (https://www.uniprot.org/). The PI and MW were calculated in Expasy (https://web.expasy.org/compute_pi/) by entering the sequences of each gene. The SMS Protein GRAVY software (https://www.bioinformatics.org/sms2/protein_gravy.html) was used to calculate the GRAVY value from the entered FASTA sequences.

A phylogenetic tree based on *B. napus* and *Arabidopsis* Ubc13 family amino acid sequences was constructed by using a maximum likelihood (ML) estimation method of a JTT matrix-based model of MEGA7.0.26. The bootstrap consensus tree inferred from 1,000 replicates. Values < 50% are omitted (parameters: Gaps/Missing data treatment -Partial deletion; Site coverage cutoff – 95%). The phylogenetic tree was exported as Newick format and opened in the Interactive Tree Of Life (iTOL), a webbased tool for phylogenetic tree manipulation and annotation (Letunic and Bork, 2021).

To identify homologs of *UBC13* family genes and the conservation of these homologous genes in *Brassicaceae*, the synteny analysis was performed among four species: *A. thaliana*, *B. napus*, *B. rapa* and *B. oleracea*. The genome assemblies for these four species were obtained from EnsemblPlants (https://plants.ensembl.org/info/data/ftp, version 55). The synteny analysis was performed by MCScanX (Wang *et al.*, 2012) with default parameters from top-five BlastP hits. Two Arabidopsis *UBC13* genes (AT1G16890 and AT1G78870) were used to search for gene pairs in three Brassica species. When performing the synteny analysis among Brassica species, the genome of *B. napus* was split into two subgenomes (A and C), with gene pairs detected between the A subgenome and *B. rapa*, and between the C subgenome and *B. oleracea*, correspondingly. Circos plot for synteny analysis was further performed through http://circos.ca/.

***B. napus UBC13* cDNAs cloning and plasmid construction**

Total RNA was extracted from *B. napus* seedlings with a TRIzol reagent and used for reverse transcriptase (RT)-PCR with the SuperScript RT-PCR III system (Invitrogen) according to manufacturer's instructions. Full length *BnUBC13* coding sequences were cloned into yeast two-hybrid (Y2H) vectors pGBT9E and pGAD424E, which were derived from pGBT9 (Gal4BD) and pGAD424 (Gal4AD) (Bartel and Fields, 1995), respectively, with a frameshift at the multiple cloning site. The identity of the cloned inserts was confirmed by DNA sequencing.

Yeast survival assays

A yeast strain HK578-10D and its isogenic mutant derivatives were transformed or co-transformed with pGBT9 and/or pGAD424 based plasmids as indicated, and at least five colonies were selected after 3-day incubation on the selective plate (SD-Leu plates for the single transformation and SD-Leu-Trp for double transformations) and streaked onto the same selective plates. For a gradient plate assay, transformed yeast cells were used to inoculate liquid SD minimal medium. Equal number of cells were taken after overnight incubation and imprinted onto YPD alone or YPD gradient plates containing 0.025% MMS gradient in the bottom layer. 0.1 mL of overnight culture was mixed with 0.4 mL of sterile distilled water and 0.5 mL of molten agar on a sterile microscopic slide and the mixture was printed on the plates across the gradient with another microscopic slide. All the plates were incubated at 30 ^{o}C for 3 days before photography.

For a serial dilution assay, overnight cultures were adjusted with equal cell density, made tenfold serial dilutions with sterile distilled water, and 5 µL of each sample was spotted to the plates containing desired concentrations of MMS or 4NQO. For the UV irradiation, samples were spotted to the YPD plates and exposed to predetermined UV irradiation doses in a 254 nM UV crosslinker (UVP). After the liquid was absorbed, the plates were incubated at 30 ^{o}C for 3 days before photography.

Spontaneous mutagenesis assay

A yeast strain DBY747 and its isogenic *ubc13Δ* derivative WXY849 were used in the spontaneous mutagenesis assay. These strains bear a *trp1-289* amber mutation that can be reverted to Trp^{+} by different mutation events (Xiao and Samson, 1993). WXY849 was transformed with pGAD-BnUbc13s and the transformants were selected on SD-Leu plates. The overnight yeast cell culture was used to inoculate 5 mL of YPD liquid medium with a final concentration of 20 cells/mL, which was incubated at 30 ^{o}C for 3 days. Cells were collected by centrifugation at 4,000 rpm,

resuspended in sterile distilled water and plated on SD-Leu to count for the total colony forming units and on SD-Leu-Trp to count for Trp^+ revertants. Spontaneous mutation rates were calculated as described (Williamson *et al.*, 1985).

Yeast two-hybrid analysis

The Y2H strain PJ69-4A was co-transformed with $Gal4_{BD}$ and $Gal4_{AD}$ constructs. SD-Leu-Trp plates were used to select the co-transformed colonies. At least five independent colonies from each co-transformation were printed onto SD-Leu-Trp plates and SD-Leu-Trp-His selective plates with different concentrations of 1,2,4 amino triazole (3-AT) to test activation of the P_{GAL1}-*HIS3* reporter gene and onto Leu-Trp-Ade plates to test activation of the P_{GAL2}-*ADE2* reporter gene. The above plates were incubated at 30 °C for the indicated time before photography.

Recombinant protein production and extraction

The *BnUBC13* open-reading frames (ORFs) were isolated from pGBT-BnUbc13s and cloned into pET30a (Novogene) as a His_6 fusion. The resulting pET-BnUbc13s were co-transformed with pGEX-AtUev1D (Wen *et al.*, 2008) into *Epicurian coli* BL21-CodonPLus (DE3)-RIL strain (Thermo Sci. 2,287,225). The transformed cells were cultured overnight in LB+Amp Kan, diluted 1:50 into fresh culture and incubated until $OD_{600\ nm}$ of 0.6-0.8. The His_6-BnUbc13s and GST-AtUev1D fusion proteins were induced by adding isopropyl-b-D-thiogalactopyranoside (IPTG) to the final concentration of 0.2 mM and the incubation continued for 6 h. The cells were harvested by 8,000 rpm centrifugation in a Beckman Coulter Avanti JA17 rotor for 1 h at 4 °C, resuspended in phosphatebuffered saline (PBS, 140 mM NaCl, 2.7 mM KCl, 10 mM Na_2HPO_4, 1.8 mM KH_2PO_4, pH 7.3), and passed through Constant Systems one shot cell disrupter at 25 PSI. The resulting crude extract was centrifuged at 17,000 rpm in the same JA17 rotor for 30 min at 4 °C, and the soluble fraction was used for the GST pulldown assay.

GST pulldown assay

The GST-pulldown assay was carried out using Glutathione Sepharose 4B Microspin™ GST purification columns as previously described (Pastushok *et al.*, 2005). Purified GSTAtUev1D and His_6-BnUbc13s were added to individual columns with glutathione beads and incubated for 1 h at 4 °C. Finally, wash buffer (1x PBS buffer with 350 mM NaCl) was used to wash the beads by running through the column. The eluted samples were subjected to 15% SDS-PAGE and visualized by Coomassie blue staining.

Ub conjugation reaction

E. coli BL21-RIL cells separately transformed with pET-BnUbc13s and pGEX-AtUev1D were incubated and induced by IPTG as described above, and the cell extracts were used for protein purification with Bio-Rad poly-prep chromatography columns (731–1550) containing Ni-NTA and glutathione beads, respectively. After washing beads with respective lysis buffers, affinity-purified recombinant proteins were eluted from the columns by using 20 mL of His6 elution buffer for His_6-BnUbc13s and GST elution buffer for GST-AtUev1D. The ubiquitination assay kit containing Ub thioester/conjugation initiation reagents was purchased from Abcam (ab139467). A 20-mL reaction mixture contained E1, Ub, MgATP, reaction buffer from the kit, plus His_6-BnUbc13 and GST-AtUev1D prepared from this study. The Ub-K63R protein was purchased from Abcam (UM-K63R). Conjugation reactions were performed at 37 °C for 4 h according to manufacturer's instructions, followed by running of 15% SDS-PAGE and western blotting using polyclonal goat anti-Ub antibodies (Bio-Rad).

9. Results and discussion: *Describe and discuss the results accomplished during the entire project period under each objective listed under section 7. The results need to be accompanied with pertinent tables, figures and/or other illustrations. Provide discussion necessary to the full understanding of the results. Where applicable, results should be discussed in the context of existing knowledge and relevant literature. Detail any major concerns or project setbacks. (**Maximum of 30 pages of text not including figures or tables**)*

Objective 1: Establish transgene-free CRISPR/Cas9 based genome editing platform

The CRISPR/Cas9 based genome-editing platform has been successfully established. This platform includes three steps: Step 1. Design and construct Cas9/sgRNAs vector targeting candidate genes. In this project, we designed eight sgRNA constructs and targeted 22 *B. napus* genes (details are shown in Objective 2.3 and 2.4); Step 2. Deliver validated Cas9/sgRNAs vectors into canola plants via Agrobacterium-mediated transformation. In this project, we obtained 198 regenerated plants through this transformation. The transformation process is shown in Figure 1.1; Step 3. Identify mutations in regenerated plants by PCR/sequencing.

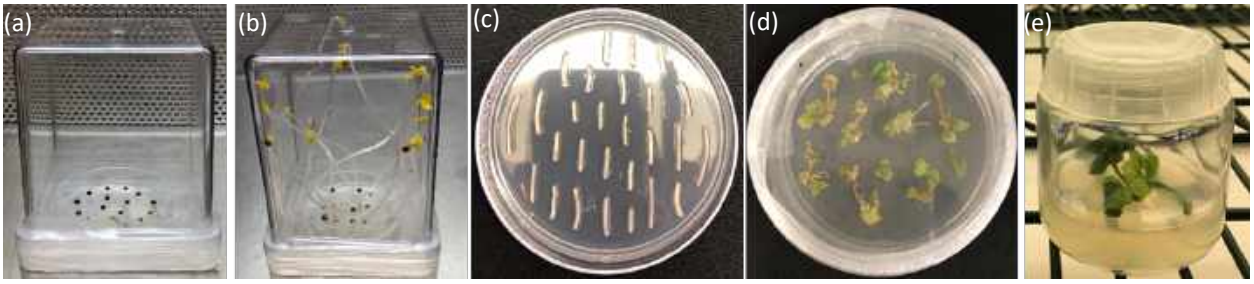

Figure 1.1. Agrobacterium-mediated canola transformation process. (a) seed germination; (b) seedling; (c) hypocotyl fragments infected with Agrobacterium; (d) calli induction; (e) shoots and roots induction.

Objective 2: Identify novel clubroot susceptibility genes and create corresponding resistance allelic variants in elite canola germplasms

Different from *R*-gene mediated disease resistance, a new alternative strategy based on susceptibility (*S*) genes has been proposed as they have the potential to be more durable in the field (Zaidi *et al.*, 2018). *S* genes can either act as negative regulators of immunity or are considered essential compatible factors for successful pathogen infection (van Schie and Takken, 2014). While *R* genes are mostly dominant, the disease resistance provided by manipulation of *S* genes is mostly recessive. Therefore, broad-spectrum disease resistance can be readily conferred by disrupting *S* genes via precise genome-editing tools (Garcia-Ruiz *et al.*, 2021).

In this project, we utilized this *S* gene strategy to improve clubroot resistance in canola. First, we investigated the role of *S* candidate genes in model plant, *Arabidopsis thalianna*. After confirming their involvement in clubroot susceptibility, we used Arabidopsis gene/protein sequence to blast *Brassica napus* reference genome database and identify their corresponding orthologous genes. Then, we used CRISPR/Cas9 genome editng tool to edit these genes in canola plants. After identifying edited mutant plants, we did clubroot disease assessment on these plants to confirm their conferred resistance to clubroot.

2.1 Arabidopsis *UBC13A* and *UBC13B* are clubroot susceptibility genes

The first two *S* candidate genes we investigated are *ubiquitin conjugating enzyme 13* (*UBC13*) genes, encoding a key enzyme responsible for Lysine (K) 63-linked polyubiquitination, a posttranslational protein modification, which regulates numerous important cellular processes in all eukaryotes (Yang and Xiao, 2022). The Arabidopsis genome contains two *UBC13* genes, *UBC13A* (At1g78870) and *UBC13B* (At1g16890) (Wen *et al.*, 2006). Subsequent studies reveal that AtUBC13s function in apical dominance (Yin *et al.*, 2007), DNA damage repair (Wen *et al.*, 2006), iron metabolism (Li and Schmidt, 2010), auxin signaling (Wen *et al.*, 2014), low temperature stress response (Wang *et al.*, 2019) and plant immunity (Wang *et al.*, 2019, Yao *et al.*, 2021). However, it is not known whether UBC13s play roles in the response to clubroot disease infection.

2.1.1 Inactivation of UBC13 *increased resistance against clubroot*

In this study, the Arabidopsis *ubc13a ubc13b* (*ubc13*) double mutant, its corresponding wild type Col-0 line (WT), and AtUBC13A-transformed *ubc13* mutant line (*AtUBC13A/ubc13*) were inoculated with *P. brassicae* pathotype 3H. At 28 days after inoculation (dpi), WT and *AtUBC13A/ubc13* plants displayed wilting and stunting phenotypes (Figure 2.1). Their rosette leaves showed stressed purple color and were all died. In contrast, *ubc13* mutant plants remained

green and grew normally. The underground part of WT and *AtUBC13A/ubc13* plants showed severe disease symptoms as well (Figure 2.2). For instance, their main roots were all destroyed or degraded by clubroot pathogen at 28 dpi. Instead, large club shaped galls formed over the root and hypocotyl and extended in part into the rosette ground (Figure 2.2). However, *ubc13* mutant showed tolerance to *P. brassicae*, as indicated by reduced swellings of the root part and remained main root (Figure 2.2).

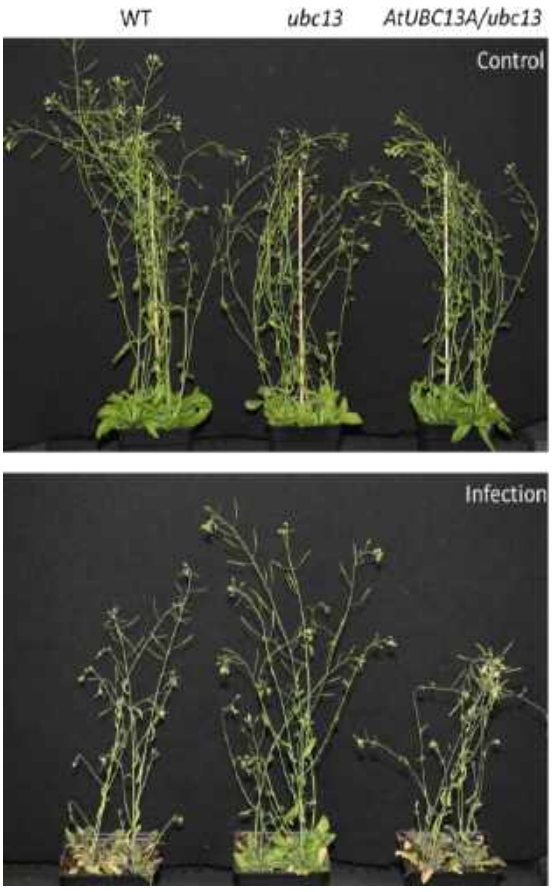

Figure 2.1 Aboveground phenotypes of plants with or without inoculating *Plasmodiophora brassicae* Pathotype 3H at 28 dpi.

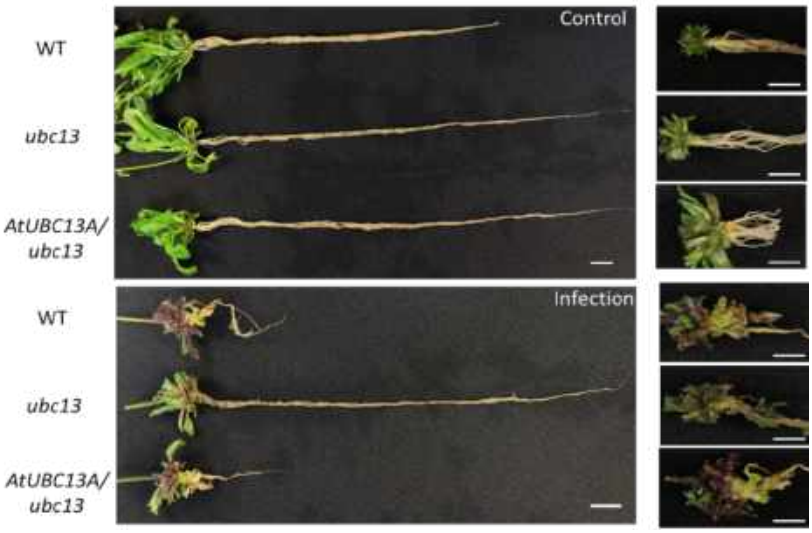

Figure 2.2 Root phenotypes of plants with or without inoculation by *Plasmodiophora brassicae* Pathotype 3H at 28 dpi.

2.1.2 Less P. brassicae zoosporangia produced in the ubc13 mutant

The clubroot resistance conferred in *ubc13* mutant encouraged us to examine whether mutant plants prevent or slow down the formation of pathogen *P. brassicae* in the infected roots. The segments of *P. brassicae*-inoculated roots of Col-0 wild type and *ubc13* mutant at 14 dpi were examined under differential interference contrast (DIC) microscopy using a confocal microscope. The epidermal cells and root hairs of *ubc13* mutant displayed much fewer zoosporangia compared to WT (Figure 2.3). This observation was confirmed by quantitative PCR that measured two *P. brassicae* housekeeping genes *Pb249* and *Pb28S* in the infected roots of WT and *ubc13* mutant. As shown in Figure 2.4, the transcript levels of both genes in *ubc13* mutant were significantly lower than that in the WT (Figure 2.4). Taken together, these results demonstrates that *P. brassicae* still can start initial infection in the root of *ubc13* mutant, whereas the formation of zoosporangia was limited or slowed down during the secondary infection.

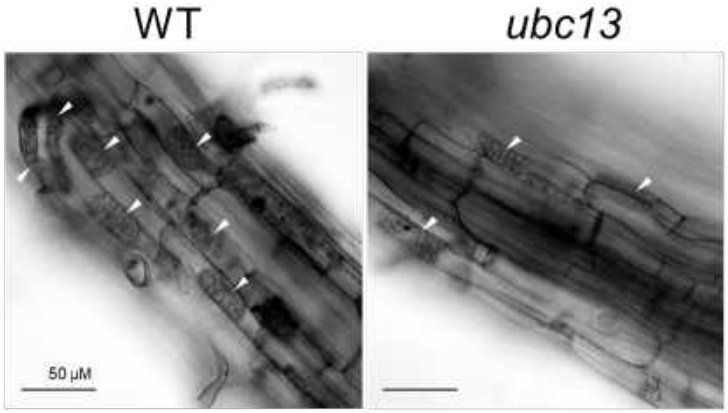

Figure 2.3 Micrographs of *P. brassicae*-inoculated roots at 14 dpi. Zoosporangia in epidermal cells and root hairs were indicated by arrowheads.

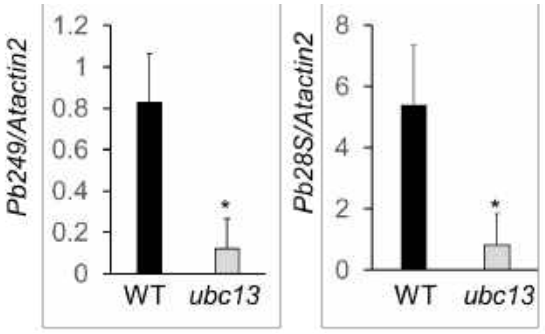

Figure 2.4 qPCR based biomass of the *P. brassicae* growth in WT and *ubc13* at 14 dpi. * $P < 0.05$

2.1.3 Inactivation of UBC13 conferred race/pathotype-independent resistance

The involvement of *UBC13* in clubroot susceptibility encouraged us to further determine if the resistance observed in the *ubc13* mutant is race/pathotype dependent. In addition to pathotype 3H, two newly identified pathotypes 5X-LG2 and 3A were employed in this study. At 28 dpi, most WT and *AtUBC13A/ubc13* plants displayed highest disease severity level with severe disease symptoms, such as big galls on the main root and hypocotyl resulting in degradation of root and eventually plant death (Figure 2.5). In contrast, 80-100% of *ubc13* plants showed intermediate disease severity against three different pathotypes. This result indicates that loss of function of *UBC13* can confer race independent resistance against multiple *P. brassicae* pathotypes.

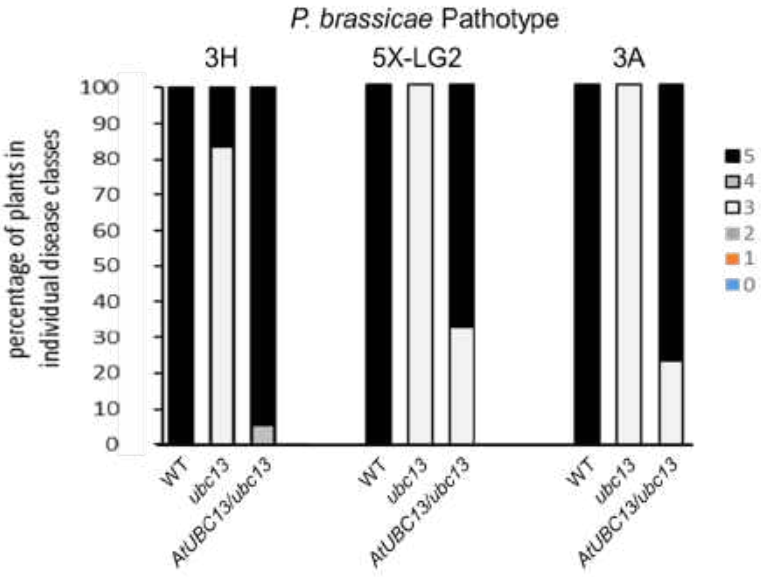

Figure 2.5 The disease severity index of clubroot in plants after soil inoculation with *P. brassicae* pathotype 3H, 5X-LG2 and 3A.

2.1.4 Metabolites profoling in WT and ubc13 mutant plants after P. brassicae inoculation

A global metabolomic profiling of WT and *ubc13* plants after *P. brassicae* inoculation was performed to determine the mechanism by which Ubc13 mediates clubroot susceptibility in Arabidopsis. Overall, 5423 metabolite

features were detected, of which 719 metabolites were high-confidently identified and annotated. Principal components analysis (PCA) showed a clear separation in genotype (30.0% of variance for principal component one) and treatment (19.9% of variance for principal component two) (Figures 2.6a). Interestingly, the variance between inoculated and control in *ubc13* was much lower compared to that in the WT, suggesting that less metabolism changes occurred in the *ubc13* plant after clubroot infection. When compared with the corresponding mock treatment, 348 and 182 differentially accumulated metabolites (DAM) were detected in the WT and *ubc13* plants with p-value < 0.05 after *P. Brassicae* inoculation, respectively. A total of 84 DAMs were detected in both genotypes, while 264 and 98 DAMs were WT specific and *ubc13* specific, respectively (Figure 2.6b).

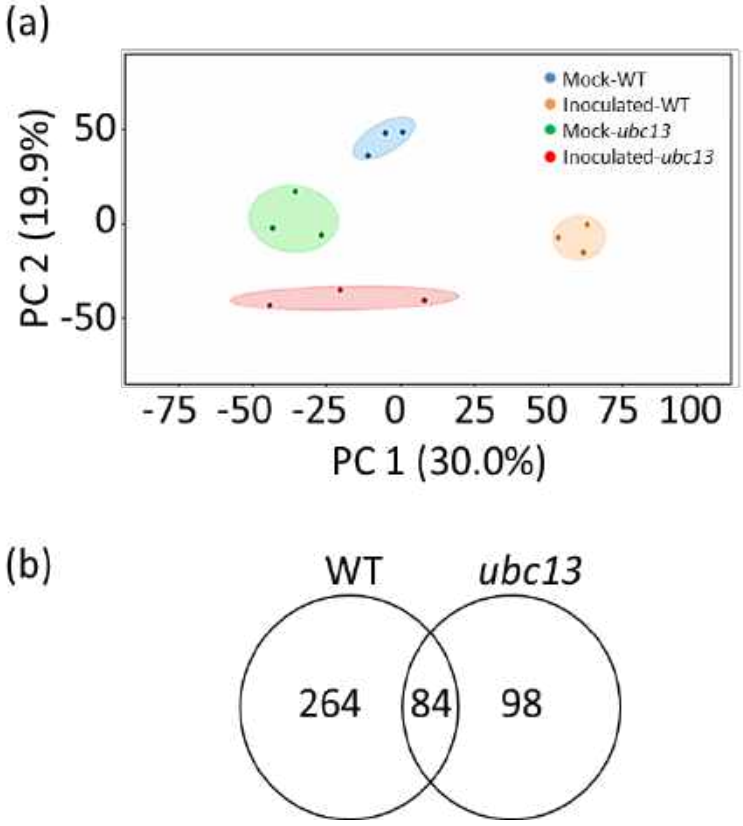

Figure 2.6 Overview of the metabolites identified using LC-MS analysis. (a) Principal Component Analysis (PCA) plots for metabolic data. (b) Venn diagram representing the number of differentially accumulated metabolites (DAM) in WT and *ubc13*. The overlapping area in the diagram represents the number of DAMs common in both genotypes.

Kyoto Encyclopedia of Genes and Genomes (KEGG) pathway enrichment analysis was performed on WT and *ubc13* DAMs. Many metabolism pathways that were previously reported to be involved in clubroot response were highly enriched in the WT, while they were less represented in the *ubc13* plants (Figure 2.7). For example, multiple amino acid biosynthesis and metabolism pathways, citrate cycle, glutathione metabolism, flavonoid biosynthesis, phenylpropanoid biosynthesis and Vitamin B6 metabolism were all enriched in both genotypes, but with different levels. To further investigate differences in the metabolic changes after infection between WT and *ubc13*, several metabolism pathways were analyzed in details.

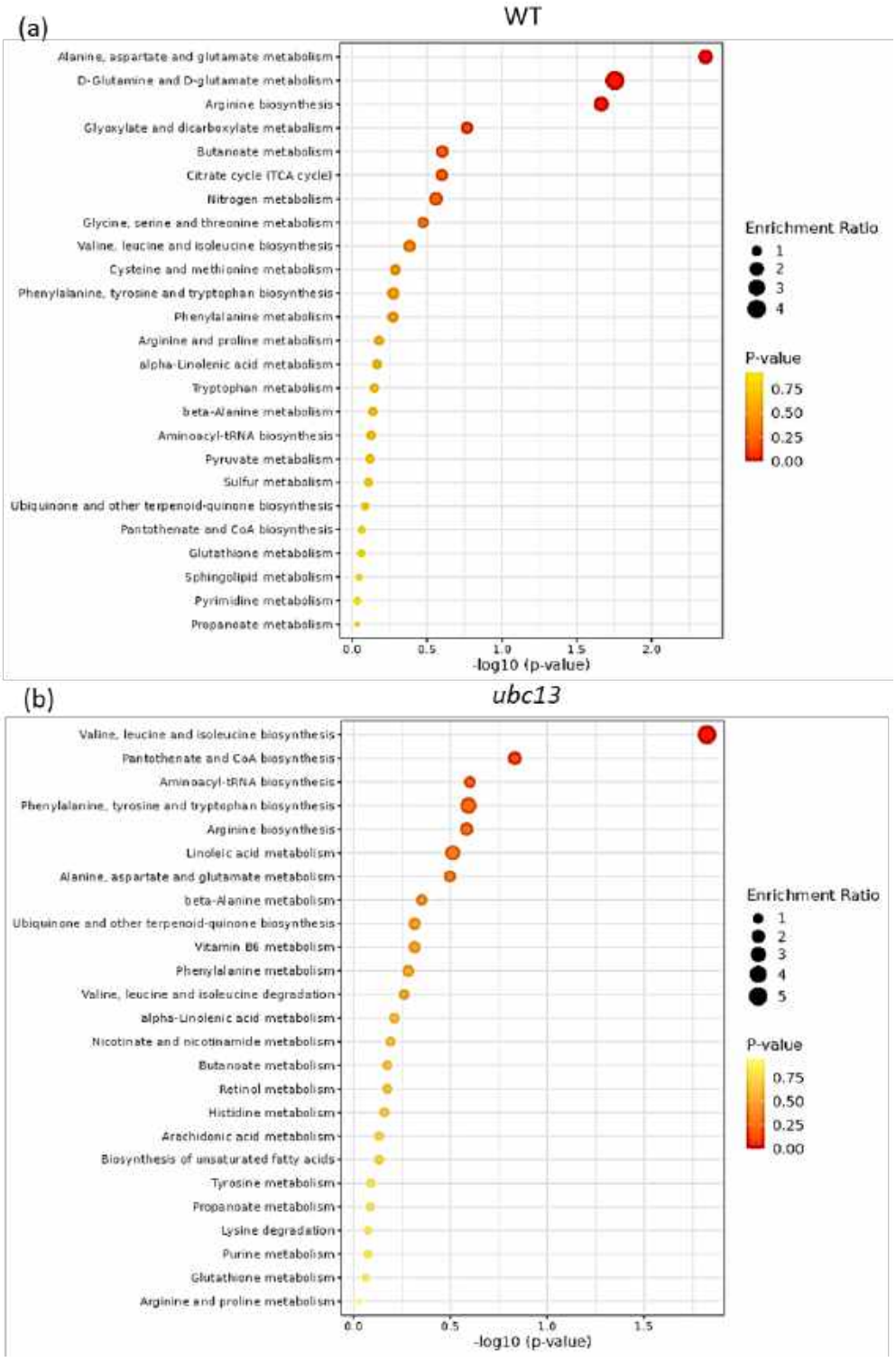

Figure 2.7 KEGG pathway enrichment analyses on differentially accumulated metabolites (DAMs) in WT (a) and *ubc13* (b).

2.1.4 Amino acid biosynthesis and metabolism changes

Clubroot infection caused significant changes in several principle amino acid biosynthesis and metabolism pathways (Ludwig-Müller *et al.*, 2009, Wagner *et al.*, 2012, Malinowski *et al.*, 2019). In total, 142 amino acid-related metabolites were identified in our DAM data. Among them, only 14 DAMs displayed similar accumulation patterns in both genotypes. 96 DAMs exclusively appeared in WT, while only 24 exclusively appeared in *ubc13*. The major free amino acids that were altered after inoculation are shown in Table 2.1. Histidine (wt: 1.7 and *ubc13*: 1.8) and Lysine (wt: 1.6 and *ubc13*: 2.2) were significantly increased in both genotypes. Arginine (1.4), Asparagine (1.2), Cystine (1.9) and Glutamine (1.3) were increased exclusively in WT, while Isoleucine (2.5), Tryptophan (1.6), Ty-rosine (1.9), Valine (1.8) and Aspartic acid (1.5) were increased exclusively in *ubc13*. Glycine was the only amino acid decreased in both genotypes (wt: 0.8 and *ubc13*: 0.8). In addition, Glutamic acid (0.7), Methionine (0.7), Serine (0.7) and Threonine (0.7) were exclusively decreased in WT.

Table 2.1 The list of free amino acids significantly changed after *P. brassicae* inoculation in WT and *ubc13* plants.

Amino acids	WT[a]	*ubc13*
Histidine	1.7*[b,c]	1.8*
Lysine	1.6*	2.2*
Arginine	1.4*	n.s.[d]
Asparagine	1.2*	n.s.
Cystine	1.9*	n.s.
Glutamine	1.3*	n.s.
Isoleucine	n.s.	2.5*
Tryptophan	n.s.	1.6*
Tyrosine	n.s.	1.9*
Valine	n.s.	1.8*
Aspartic acid	n.s.	1.5*
Glycine	0.8*	0.8*
Glutamic acid	0.7*	n.s.
Methionine	0.7*	n.s.
Serine	0.7*	n.s.
Threonine	0.7*	n.s.

[a]The values represent "Fold Change" showing the ratio of the average peak value (^{12}C-labeled individual sample *vs*. ^{13}C-labeled pool) in inoculation to that in the control.
[b]* indicates $P<0.05$
[c]Values in red indicate upregulation; in green indicate down-regulation.
[d]n.s. no signification change

2.1.5 The metabolites of tricarboxylic acid (TCA) cycle

The TCA cycle is crucial for cellular energy and carbon skeleton supply, especially for sugar catabolism (Zhang and Fernie, 2018). Upregulation of TCA cycle genes were reported in the infected Arabidopsis root (Schuller *et al.*, 2014, Irani *et al.*, 2018). The amount of five key intermediates in the TCA cycle including Citrate (1.1), Oxaloacetate (OAA, 1.5), Fumarate (1.4), L-Malate (1.5), and Alpha-Ketoglutaric acid (2OG, 0.8) were significantly changed in the infected WT but not in *ubc13* roots after inoculation (Figure 2.8).

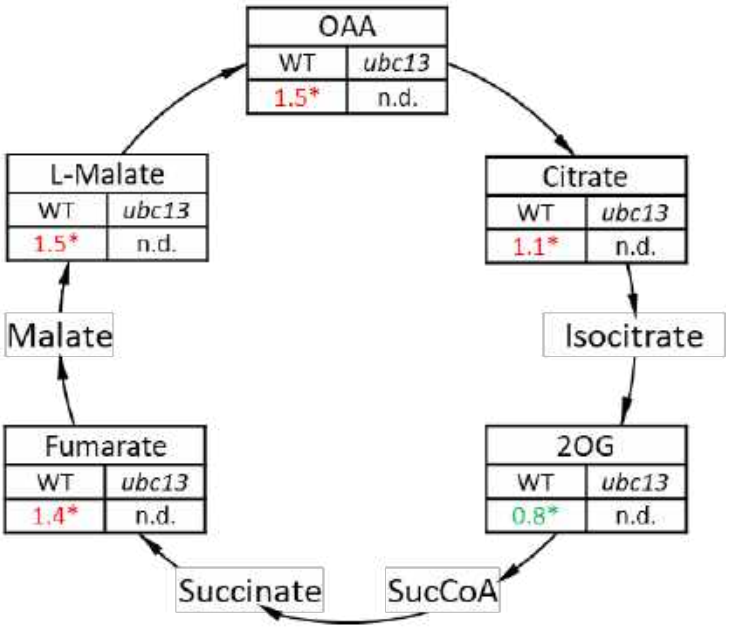

Figure 2.8 The change of metabolites of TCA after *P. brassicae* inoculation in WT and *ubc13* mutant. The values represent "Fold change" showing the ratio of the average peak value (^{12}C-labeled individual sample *vs*. ^{13}C-labeled pool) in inoculation to that in the control. * indicates *P*<0.05. Values in red indicate upregulation and green indicate down-regulation. n.d. no signification difference.

2.1.6 UBC13 is required for P. brasssicae induced auxin responsive gene expression

Clubroot symptoms were reported to be correlated with the increase in auxin (Ludwig-Müller *et al.*, 2009). Auxin responsive genes were induced after clubroot infection (Siemens *et al.*, 2006, Jahn *et al.*, 2013). The auxin signalling pathway has been considered as a susceptible factor that contributes to the clubroot disease development. Coincidently, our previous study revealed that Ubc13 contributes to the root development by affecting the auxin signaling pathway (Wen *et al.*, 2014). The *ubc13* mutant plants were insensitive to auxin treatments (Wen *et al.*, 2014). These studies imply that Ubc13 participates in the clubroot susceptibility though regulating auxin signaling. To examine this hypothesis, the transcripts of several auxin signaling and responsive genes were measured after *P. brassicae* inoculation. Among them, Indole-3-acetic acid inducible gene (*IAA29*; At4g03400), auxin responsive GH3-related gene (*Dwarf in light 2, DFL2*; At4g03400), and auxin efflux carrier gene (*PIN-FORMED 2*, *PIN2*; At5g57090) were significantly induced in WT but not in *ubc13* mutant (Figure 2.9). This result indicates that Ubc13 regulates auxin gene induction during clubroot infection.

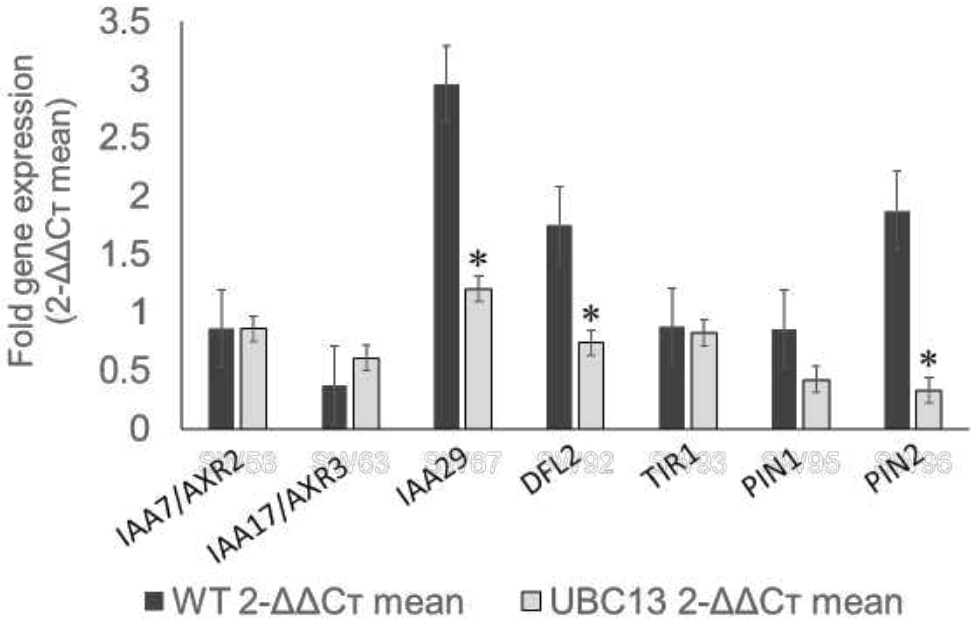

Figure 2.9 qRT-PCR data of relative gene expression ($2^{-\Delta\Delta Ct}$) for WT and *ubc13* at 14 dpi. The expression levels were normalized to the transcript level of the *A. thaliana* actin gene, and the relative transcript levels of auxin responsive genes were calculated using the comparative threshold ($2^{-\Delta\Delta Ct}$) method. The transcript level of genes in WT (Col-0) was standardized to 1. Values represent the mean±SE of three independent biological replicates, and each biological replicate contained three technique replicates. Student's t test, *p< 0.05.

2.2 Molecular characterization of *Brassica napus UBC13* genes

Our study in Arabidopsis indicates that *UBC13* is a susceptible factor and contributes to clubroot disease infection, making it an ideal target for gene eiting in canola to improve clubroot resistance. First of all, we searched and identified orthologous *UBC13* genes in *Brassica napus*. Then, we employed a yeast cell system to functionally validate if *BnUBC13* genes have typical Ubc13 functions that have been well characterized in other eukaryotes.

2.2.1 Identification and bioinformatics analyses of Brassica napus UBC13 genes

To identify *B. napus UBC13* genes, the Arabidopsis Ubc13 protein sequence was used to Blast the *B. napus* protein database (https://plants.ensembl.org/Brassica_napus/Tools/Blast). Eight predicted highly similar proteins (E-values at or below 10^{-56}), namely BnaA06g11360D (GenBank accession OP380669), BnaC08g38130D (OP380670), BnaAnng13030D (OP380671), BnaC08g17090D (OP380672), BnaA07g34450D (OP380673), BnaA08g23450D (OP380674), BnaC05g12900D (OP380675) and BnaC06g39290D (OP380676), were found and named as BnUbc13A-H, respectively. In addition, four predicted incomplete proteins in the database, BnaC02g25260D (OP380677), BnaA07g38410D (OP380679), BnaC06g20310D (OP380678) and BnaA02g19070D (OP380680), have about 99% sequence identity with AtUbc13. After cDNA amplification and sequencing, these four encoded proteins were also found to be highly homologous to AtUbc13 and subsequently named BnUbc13I-L. Features of the 12 identified *BnUBC13* genes and gene products, including number of exons, gene location, protein domain and length, molecular weight (MW), isoelectric point (pI) and grand average of hydropathicity index (GRAVY), are summarized in Table 2.2.

Table 2.2 The characteristics of identified *Brassica napus UBC13* genes and gene products

Gene Name	Gene ID	Exon No.	Chr.	Genome location (bp)	Protein domain	Subcellular localization	Protein length	MW(Da)	pI	GRAVY
BnUBC13A	BnaA06g11360D	8	A06	344,258-346,977	Ubc-E2	Nucleus	153	17219.87	6.74	-0.319
BnUBC13B	BnaC08g38130D	8	C08	785,710-787,683	Ubc-E2	Nucleus	153	17219.87	6.74	-0.319
BnUBC13C	BnaAnng13030D	8	A	2,809-4,846	Ubc-E2	Nucleus	153	17205.85	6.74	-0.320
BnUBC13D	BnaC08g17090D	8	C08	1,325,895-1,327,721	Ubc-E2	Nucleus	153	17205.85	6.74	-0.320
BnUBC13E	BnaA07g34450D	8	A07	589,771-591,755	Ubc-E2	Nucleus	153	17191.82	6.74	-0.322
BnUBC13F	BnaA08g23450D	8	A08	1,018,769-1,020,653	Ubc-E2	Nucleus	153	17233.90	6.74	-0.305
BnUBC13G	BnaC05g12900D	8	C05	157,271-159,450	Ubc-E2	Nucleus	153	17220.86	6.14	-0.319
BnUBC13H	BnaC06g39290D	8	C06	1,242,282-1,244,366	Ubc-E2	Nucleus	153	17207.82	6.74	-0.339
BnUBC13I	BnaC02g25250D	8	C02	55,248-55,820	Ubc-E2	Nucleus	153	17219.87	6.74	-0.319
BnUBC13J	BnaA07g38410D	8	A07	11,368-13,148	Ubc-E2	Nucleus	153	17219.87	6.74	-0.319
BnUBC13K	BnaC06g20310D	8	C06	952,275-954,207	Ubc-E2	Nucleus	153	17191.82	6.74	-0.322
BnUBC13L	BnaA02g19070D	8	A02	411,743-413,324	Ubc-E2	Nucleus	153	17219.87	6.74	-0.319

None of the predicted BnUbc13 proteins contains a trans-membrane domain

All 12 BnUbc13 proteins contain 153 amino acids and their alignment with AtUbc13s is shown in Figure 2.9a. AtUbc13A and AtUbc13B differ by only two conserved amino acids (Wen *et al.*, 2006). Within BnUbc13s, BnUbc13A, B, I, J and L are identical to AtUbc13B; BnUbc13C and D are identical to each other but differ from AtUbc13B by one amino acid; BnUbc13E and K are identical to each other but differ from AtUbc13B by two amino acids; BnUbc13G, F and H differs from AtUbc13B by 1, 2 and 3 amino acids, respectively. These amino acid substitutions do not affect known functional residues, including M66 (blue asterisk) involved in physical interaction with E3s (Wooff *et al.*, 2004), E57, F59 and R72 (Pastushok *et al.*, 2005) required for the interaction with UEV, and the active site C89 to conjugate Ub (Hofmann and Pickart, 1999). All BnUbc13s appear to be closer to AtUbc13B in sequence than to AtUbc13A, as the two amino acid variations in AtUbc13A were not found in any BnUbc13s (Figure 2.10a).

The phylogenetic analysis of BnUbc13s to AtUbc13s was performed. As shown in Figure 2.10b, all 12 BnUbc13s can be grouped into two clades separately derived from AtUbc13A and AtUbc13B, and the bootstraps in the clade of AtUbc13B are higher than that of AtUbc13A. To further assess the conservation of *BnUBC13* genes in Brassicaceae, we performed synteny analysis among four related species: *A. thaliana*, *B. napus*, *B. rapa* and *B. oleracea*. As anticipated, the *B. napus* genome was split into two subgenomes A and C, corresponding to *B. rapa* and *B. oleracea* genomes, respectively (Figure 2.11).

(a)

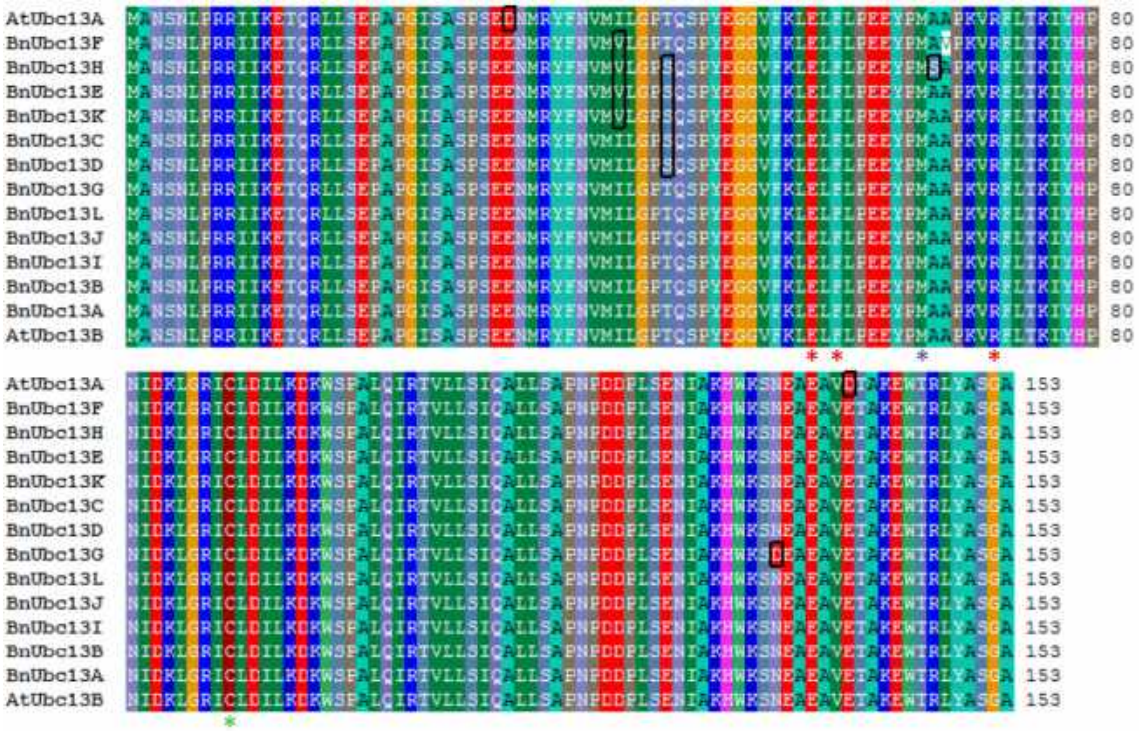

(b)

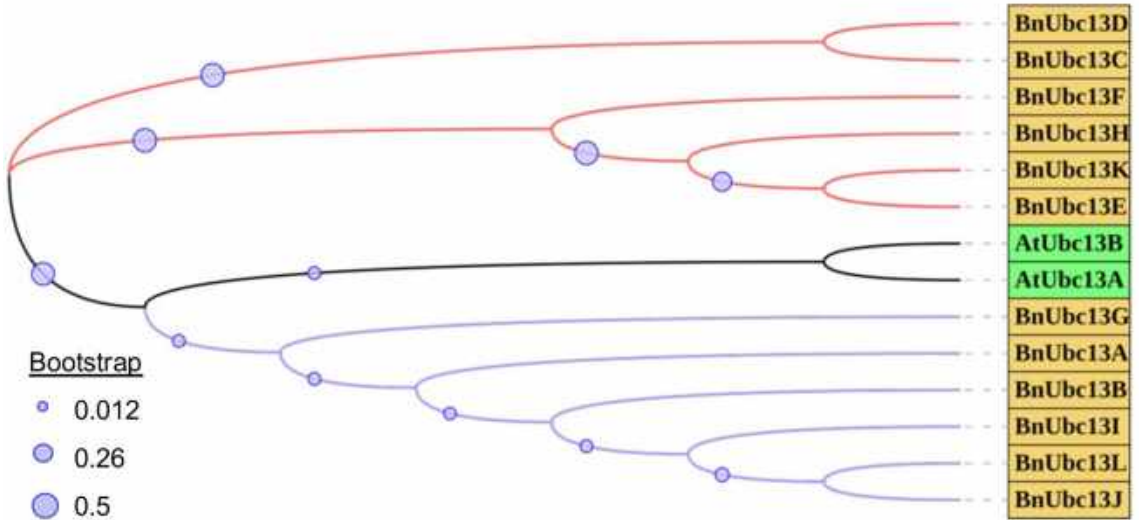

Figure 2.10 Sequence analysis of Ubc13s from *B. napus* (Bn) and *A. thaliana* (At). (a) Predicted amino acid sequences of *UBC13* gene products from *B. napus* and Arabidopsis were aligned by the BioEdit software version 7.2.5. Identical residues shared by the majority of Ubc13s are highlighted. Amino acid residues required for the interaction with UEV are marked by red asterisks, required for the interaction with a RING E3 is marked by a blue asterisk, and the active site Cys residue is marked by a green asterisk. (b) A phylogenetic tree based on *B. napus* and Arabidopsis Ubc13 family amino acid sequences was constructed by using MEGA7.0.26 and iTOL. Lines with different colors represent different branches: black, Arabidopsis; red and purple, two separate branches of *B. napus*. Yellow and green rectangles highlight Ubc13 proteins from *B. napus* and Arabidopsis, respectively. Purple circles indicate bootstrap levels as indicated.

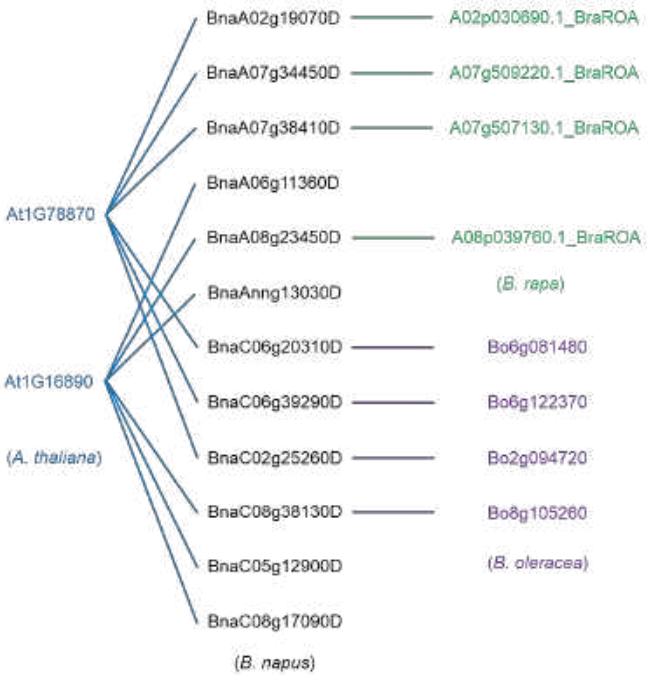

Figure 2.11 Synteny analysis of *UBC13* family genes among *Arabidopsis thaliana*, *Brassica napus*, *B. rapa* and *B. oleracea*. Identified gene pairs were linked by solid lines with different colors: blue, between *A. thaliana* and *B. napus*; green, between A subgenome of *B. napus* and *B. rapa*; purple, between C subgenome of *B. napus* and *B. oleracea*. *UBC13* family genes from different species were labeled with different colors.

2.2.2 Functional complementation of yeast ubc13 null mutants by BnUBC13s

Budding yeast *UBC13* functions in the error-free DNA damage tolerance (DDT) pathway (Broomfield *et al.*, 1998, Brusky *et al.*, 2000, Fan *et al.*, 2020). To ask whether *BnUBC13*s have same functions as yeast *UBC13*, pGBT-BnUBC13 plasmids were transformed into the yeast *ubc13Δ* mutant and cell survival in the presence of various DNA-damaging agents were examined by a serial dilution assay. As previously reported (Brusky *et al.*, 2000), the yeast *ubc13* mutant displayed an increased sensitivity to a variety of DNA-damaging agents including methyl methanesulfonate (MMS), 4-nitroquinoline 1-oxide (4NQO) and ultraviolet (UV) irradiation, while expression of *BnUBC13*s could functionally complement the yeast *ubc13* DDT defect (Figure 2.12a). Similarly, in a gradient plate assay, deletion of *UBC13* resulted in an increased sensitivity to MMS, while pGBT-BnUBC13s, but not the pGBT9 empty vector, were able to restore cellular resistance to MMS (Figure 2.12b).

Yeast *UBC13* functions in an error-free DDT pathway in parallel to the translesion DNA synthesis (TLS) pathway in response to lesions that block replication (Brusky *et al.*, 2000). While mutations in each pathway cause moderate sensitivity to DNA damaging agents, double mutations defective in both pathways result in synergistic effects (Xiao *et al.*, 1999). Figure 2.13 shows that in the presence of 0.001% MMS, neither *ubc13Δ* nor *rev3Δ* single mutant displayed increased sensitivity; however, the *ubc13Δ rev3Δ* double mutant did not grow at all in the gradient plat assay. Under the same experimental conditions, expression of any of the eight *GAL4$_{BD}$-BnUBC13* genes, but not GAL4$_{BD}$ alone, was able to rescue the double mutant to the level indistinguishable from the wild-type or single mutants (Figure 2.13). The above observations collectively demonstrate that *B. napus UBC13* genes can functionally complement the yeast *ubc13Δ* mutant from killing by DNA-damaging agents.

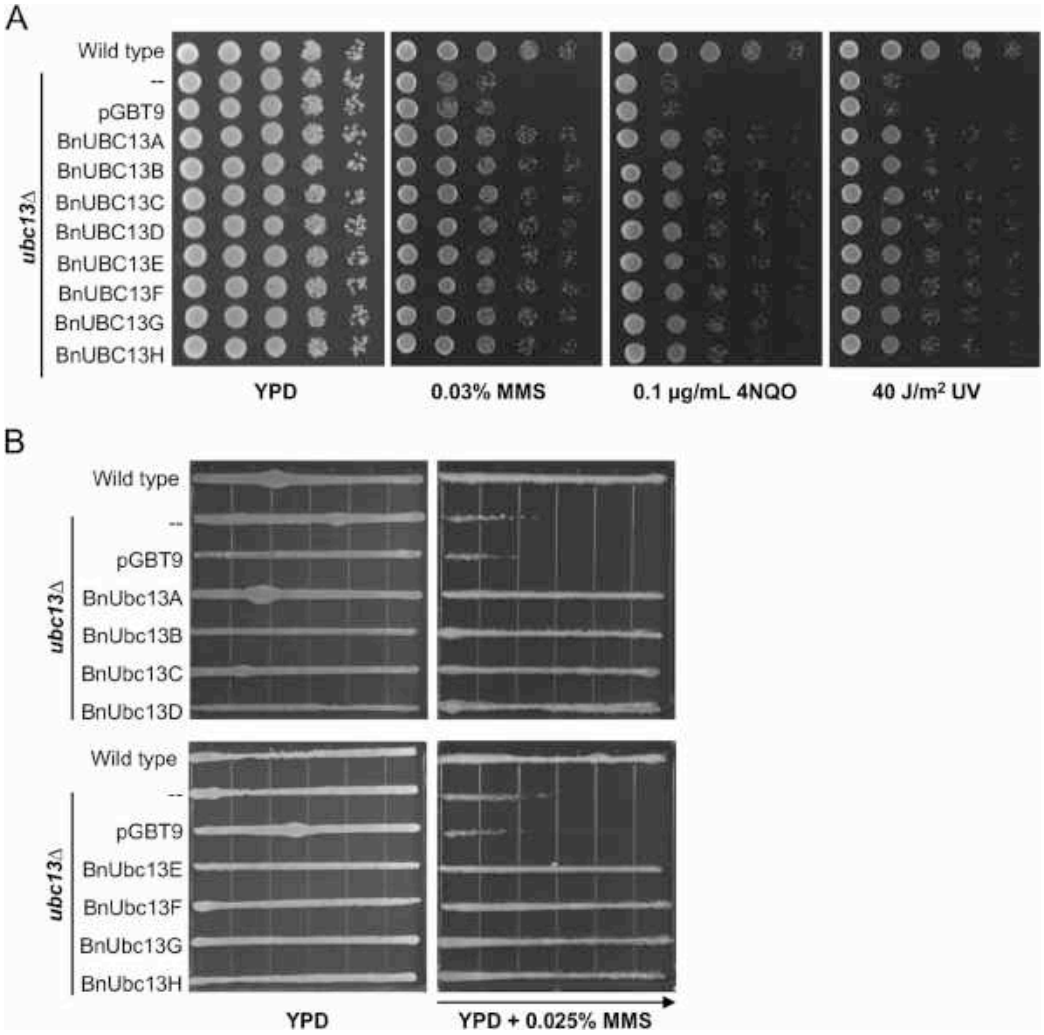

Figure 2.12 Functional complementation of the yeast *ubc13* null mutant by *BnUBC13*s. WXY904 (*ubc13Δ*) cells transformed with vector pGBT9E or plasmids carrying indicated *BnUBC13* genes were grown in the selective medium overnight and the cell density was adjusted. (a) A serial dilution assay. Cells were diluted and printed onto YPD plates with or without different concentrations of 4NQO or MMS. For the UV irradiation, plates containing printed cells were exposed to 254 nm UV at given doses. (b) A gradient plate assay. Cells were printed to a square plate across the MMS gradient at given concentrations. The plates were incubated at 30 °C for 2 days before being photographed. The arrow points to increasing MMS concentrations. Several doses of DNA-damaging agents were examined and only one representative plate is shown. For each sample, several independent colonies from each transformation were examined with comparable results, and only one set of plates is shown. Wild type, HK578-10D

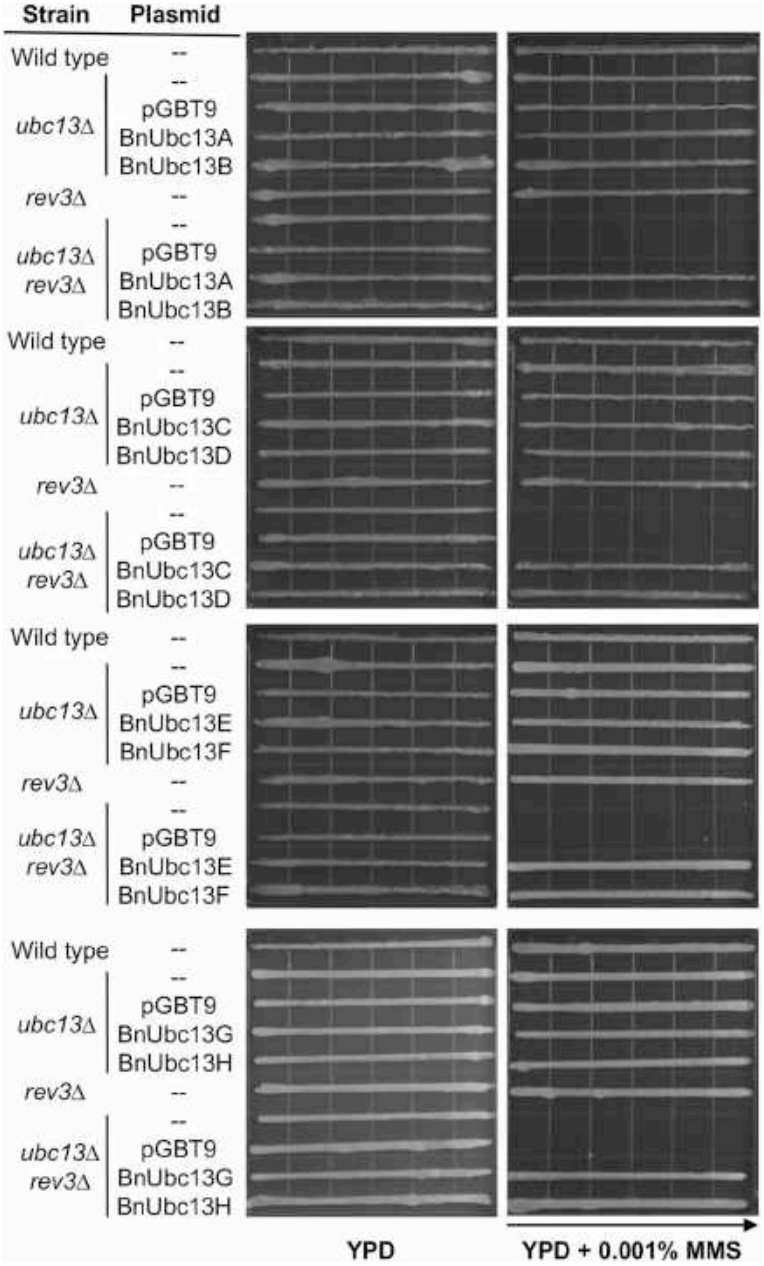

Figure 2.13 Functional complementation of the yeast *ubc13 rev3* double mutant by *BnUBC13*s. WXY904 (*ubc13Δ*) and WXY921 (*ubc13Δ rev3Δ*) cells transformed with vector pGBT9E or plasmids carrying indicated BnUBC13 genes were grown in the selective medium overnight. After adjustment of the cell density, cells were printed onto plates containing different concentrations of MMS gradient, and the plates were incubated at 30 ^{o}C for 2 days before being photographed. The arrow points to increasing MMS concentrations. Several independent colonies from each transformation were examined with comparable results, and only one set of plates is shown here. Wild type, HK578-10D; *rev3Δ*, WXY1233.

2.2.3 BnUBC13 genes protect ubc13 cells from spontaneous mutagenesis

Yeast *UBC13* is a member of the error-free DDT pathway and plays an important role in protecting yeast cells from spontaneous mutagenesis (Broomfield *et al.*, 1998, Brusky *et al.*, 2000). Therefore, a spontaneous mutagenesis assay was performed to determine whether *BnUBC13*s could functionally complement the error-free DDT defect in the yeast. It was apparent from Figure 2.14 that inactivation of *UBC13* in wild-type yeast cells caused nearly 27-fold increase in the spontaneous mutation rate. The large increase in spontaneous mutagenesis supports a notion that *UBC13* plays a vital role in maintaining host genome stability. In contrast, when *ubc13Δs* cells were transformed with *BnUBC13*s, the spontaneous mutation rate dropped to near wild-type levels. These results indicate that BnUbc13s can replace Ubc13 in yeast cells to limit endogenous DNA-damage stress.

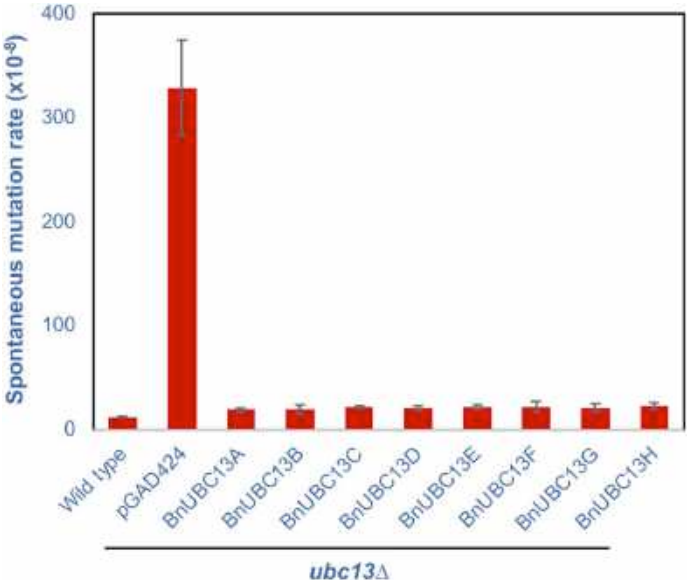

Figure 2.14 Effects of *BnUBC13s* on spontaneous mutagenesis. WXY849 (*ubc13Δ*) cells transformed with vector pGAD424E or plasmids carrying *BnUBC13* genes were grown in the selective medium, diluted in YPD, incubated at 30°C for 3 days, plated onto SD-Leu and SD-Leu-Trp, and the plates were incubated for 3 days before counting number of colonies. Spontaneous mutation rates were calculated (Williamson *et al.*, 1985) and presented as mutation events per cell per generation. Wild type, DBY747.

2.2.4 Physical interactions of BnUbc13s with AtUev1D

One condition for the yeast Ubc13 function is that it has to form a stable complex with Mms2, the only known UEV in yeast cells (Hofmann and Pickart, 1999). The fact that BnUbc13s can replace yeast Ubc13 in spontaneous and DNA-damage induced functions indicates that it must interact with Mms2 in yeast cells. To ask whether BnUbc13s are also able to interact with plant UEVs, a yeast two hybrid (Y2H) assay (Fields and Song, 1989) was employed to analyze the protein-protein interaction between BnUbc13s and AtUev1D. All eight $Gal4_{BD}$-BnUbc13s gave positive results with $Gal4_{AD}$-AtUev1D under high stringency (SD-His + 3-AT and SD-Ade) conditions in comparison to negative controls including $Gal4_{BD}$-BnUbc13s with $Gal4_{AD}$ and $Gal4_{BD}$ with $Gal4_{AD}$-AtUev1D (Figure 2.15). All the above interactions are deemed robust and strong, and no difference in the interaction strength among BnUbc13s was observed. Indeed, these interactions seem to be specific between BnUbc13s and AtUev1D as neither of the proteins alone was able to activate reporter genes in the Y2H assay. Therefore, results from the Y2H assay indicate that all BnUbc13s are able to physically interact with AtUev1D.

The physical interaction between BnUbc13 and AtUev1D was further confirmed independently *in vitro* by a GST-affinity pulldown assay. In this experiment, bacterial cells were transformed with both His_6-tagged BnUbc13s and GST-tagged AtUev1D, and the produced proteins in bacterial cells were copurified by adding to a column containing glutathione beads. After incubation, washing and elution, all eight His6-BnUbc13s were found to be co-eluted with GST-AtUev1D, but not with GST (Figure 2.16). Hence, all BnUbc13s can form stable heterodimers with AtUev1D *in vitro*.

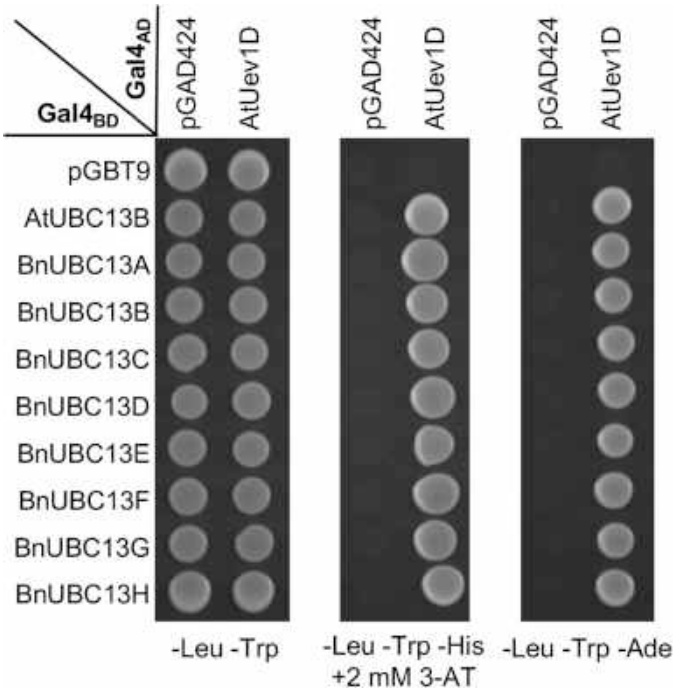

Figure 2.15 Physical interactions between BnUbc13s and AtUev1D in a yeast two-hybrid assay. PJ69-4A cells co-transformed with vectors pGBT9E ($Gal4_{BD}$) and pGAD424E ($Gal4_{AD}$) or plasmids carrying *AtUEV1D* and indicated BnUBC13s were grown in the SD-Leu-Trp medium overnight. After adjustment of cell density, cells were replicated on SD-Trp-Leu (control), SD-Trp-Leu-His plus various concentrations of 3-AT, and SD-Trp-Leu-Ade, followed by incubation for 3 days at 30 ^{o}C before being photographed. Five independent colonies from each transformation were examined with comparable results, and only one set is shown here.

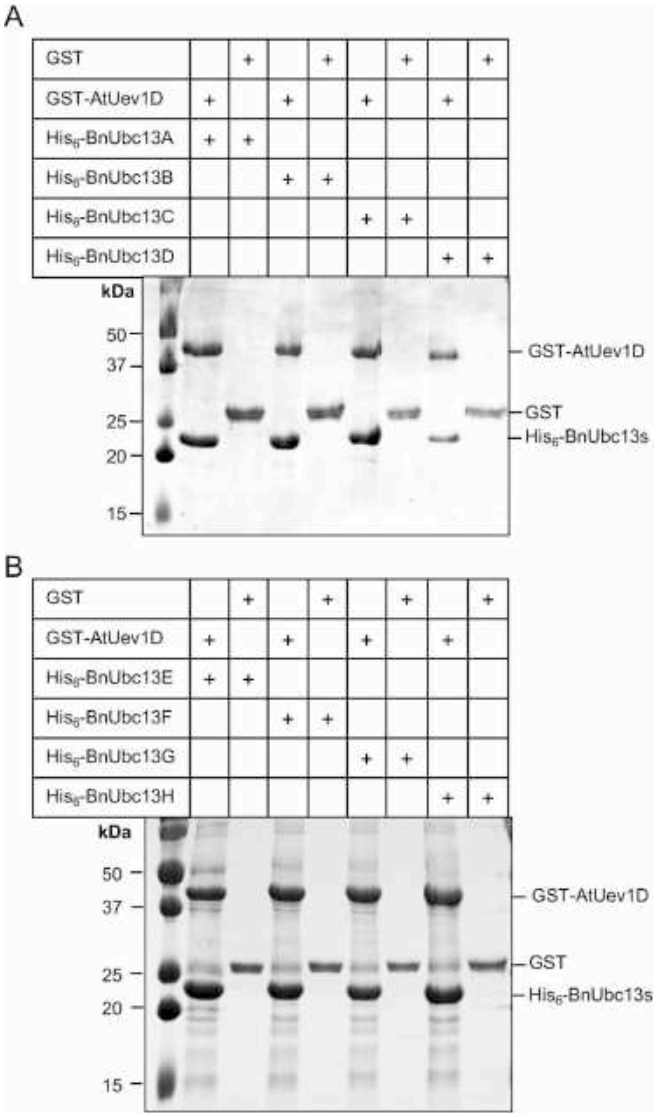

Figure 2.16 Physical interactions between BnUbc13s and AtUev1D in a GST pulldown assay. Co-purified GST-AtUev1D and His_6-BnUbc13s were added to microspin columns. After incubation and washing, the columns were eluted with reduced glutathione and subjected to SDS-PAGE analysis. (a) AtUev1D with BnUbc13A-D. (b) AtUev1D with BnUbc13E-H. Identities of key bands are marked.

2.2.5 Dual rescue of yeast ubc13 mms2 by BnUBC13s and AtUEV1D

To assess *in vivo* complex formation and functions between BnUbc13s and AtUev1D, the *ubc13 mms2* double mutant was created and co-transformed with pGBT-BnUBC13s and pGAD-AtUEV1D, or with their respective empty vectors. When the double mutant cells were transformed with only pGBT-BnUBC13s or pGAD-AtUEV1D, the transformed cells did not display enhanced resistance to MMS (Figure 2.17), implying that both Ubc13 and UEV are required for the DDT function. In contrast, double mutant cells carrying both pGBT-BnUBC13 and pGAD-AtUEV1D plasmids displayed MMS resistance comparable to the wildtype level (Figure 2.17). Since *BnUBC13s* and *AtUEV1D* can jointly complement *ubc13Δ* and *mms2Δ* defects in yeast, one can envisage that BnUbc13s must be able to bind AtUev1D in

yeast cells to form a functional E2 complex and promote K63-linked polyubiquitination on PCNA (Hoege *et al.*, 2002), which is a highly conserved process within eukaryotes including plants (Yang and Xiao, 2022).

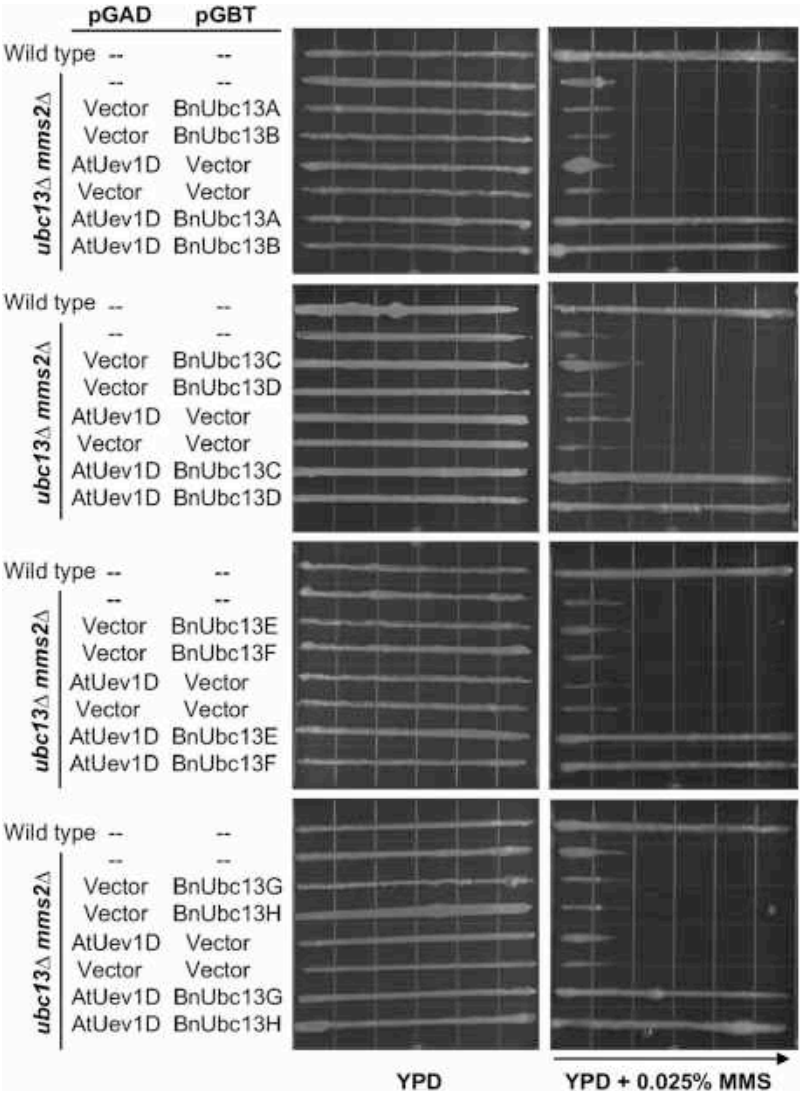

Figure 2.17 Functional complementation of the yeast *ubc13 mms2* double mutant by *BnUBC13s* and *AtUEV1D*. WXY955 (*ubc13Δ mms2Δ*) cells co-transformed with vectors pGBT9E and pGAD424E or with plasmids containing *AtUEV1D* and indicated *BnUBC13s* were grown in the SD-Leu-Trp selective medium overnight. After adjustment with cell density, cells were printed onto YPD plates containing 0.025% MMS gradient and the plates were incubated at 30 °C for 2 days before being photographed. The arrow points to increasing MMS concentrations. Several independent colonies from each transformation were examined with comparable results, and only one set of plates is shown here. Wild type, HK578-10D.

2.2.6 BnUbc13 mediates K63-linked polyubiquitination with AtUev1 in vitro

To directly examine whether BnUbc13s can promote K63-linked poly-Ub chain assembly, we performed an *in vitro* Ub conjugation assay with selected BnUbc13s. To date, Ubc13 is the only known E2 capable of catalyzing K63-

linked polyubiquitination; however, Ubc13 alone is insufficient and requires a UEV as a cofactor (Hofmann and Pickart, 1999). As shown in Figure 2.18, in our reconstituted Ub conjugation assay, neither BnUbc13s alone (Figure 2.18a, lanes 2, 6 and 10; Figure 2.18b, lanes 3 and 7) nor AtUev1D alone (Figure 2.18a, lanes 3, 7 and 11; and Figure 2.18b, lanes 3 and 7) was able to catalyze the poly-Ub chain formation. When both BnUbc13s and AtUev1D are present (Figure 2.18a, lanes 1, 5 and 9; Figure 2.18b, lanes 1 and 5), free poly-Ub chains are formed. These poly-Ub chains are deemed to be K63-linked, since when Ub was replaced by Ub-K63R, the poly-Ub chain formation was completely abolished (Figure 2.18a, lanes 4, 8 and 12; Figure 2.18b, lanes 4 and 8). These results demonstrate that BnUbc13s and AtUev1D can jointly form K63-linked poly-Ub chains *in vitro*.

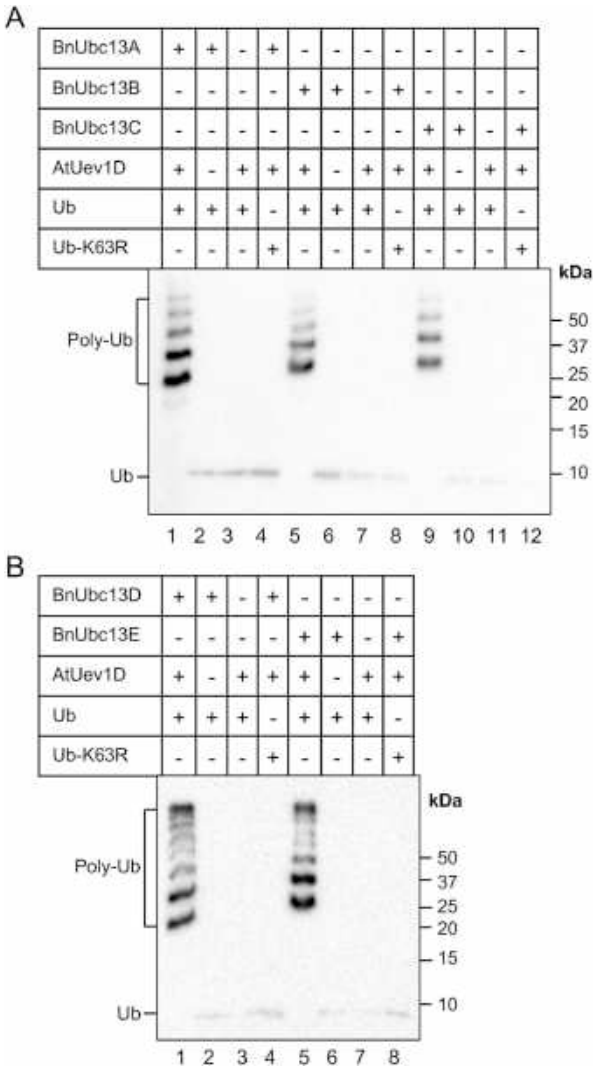

Figure 2.18 The *in vitro* Ub conjugation assay using purified BnUbc13s and AtUev1D. (a) Ub conjugation by BnUbc13A, B, C and AtUev1D. (b) Ub conjugation by BnUbc13D, E and AtUev1D. An *in vitro* Ub conjugation assay was performed using purified proteins as indicated. Assay samples were subjected to SDS-PAGE and western blotting analyses using an anti-Ub antibody. Free Ub and poly-Ub chains are marked.

2.3 Generate *Bnubc13* mutant plants via CRISPR/Cas9 based gene editing

After gene characteriation and functional validation, we attempted to create mutations in these *BnUBC13* genes via CRISPR/Cas9 based gene editing. Based on their DNA sequences, we designed four sgRNA constructs in exons 1 and 2 regions to cover all 12 genes and assembled into CRISPR/Cas9 vector separately (Figure 2.19). Completely knocking out *ubc13* gene caused lethality in some species, such as mouse (Fukushima *et al.*, 2007) and Arabidopsis (Yao *et al.*, 2021). To avoid this consequence, each sgRNA construct was individually transformed into *B. napus* line DH12075 by using Argobacterium mediated hypocotyl transformation.

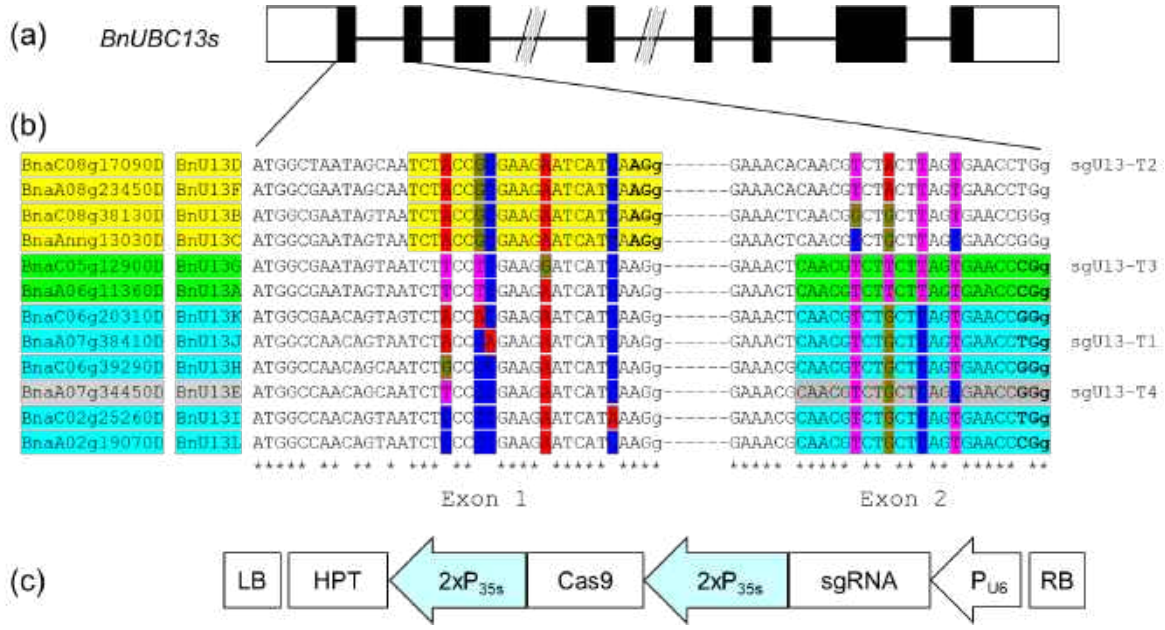

Figure 2.19 sgRNA design and CRISPR/Cas9 vector construction. (a) The *BnUBC13* gene structure includes 8 exons (filled box) separated by 7 introns (represented by the solid line) and two untranslated region (open box). (b) The alignment of first and second exon sequences of *BnUBC13* genes. The genes and sequence targeted by the same sgRNA construct was highlighted with the same color: sgU13T1 targets *BnUBC13H*, *I*, *J*, *K* and *L*; sgU13T2 targets *BnUBC13B*, *C*, *D* and *F*; sgU13T3 targets *BnUBC13A* and *G*; sgU13T4 targets *BnUBC13E*. The single nucleotide polymorphisms (SNPs) over sgRNA targeting region were indicated by different colors. Identical nucleotides were indicated by asterisks below the sequences. (c) Diagram illustrating the assembly of CRISPR/Cas9 construct: a hygromycin resistance cassette consisting of the hygromycin phosphotransferase (HPT) coding sequence driven by the cauliflower mosaic virus 35S promoter, a Cas9 expression cassette comprising the sequence encoding Cas9 driven by P35S and sgRNA driven by the U6 promoters from Arabidopsis.

The first transformed sgRNA construct sgU13-T1 can target five *BnUBC13* genes including *BnUBC13H*, *I*, *J*, *K* and *L* (Figure 2.19b). Transformation was carried out with approximately 400 hypocotyl pieces from 50 seedlings, yielding 78 independent putative transformants, of which 38 T_0 shoots formed roots after transferring to soil, grew into a mature plant and successfully generated seeds. To narrow down candidate lines for mutation analysis, a clubroot disease severity assessment was perfomed on T_1 plants of these lines. Compared to non-transformed control plants, 23 out of 38 lines significantly (P<0.01) reduced disease severity against clubroot *P. brassica* pathotype 3H (Figures 2.20 and 2.21). These 23 lines were further used for gene editing mutation analysis.

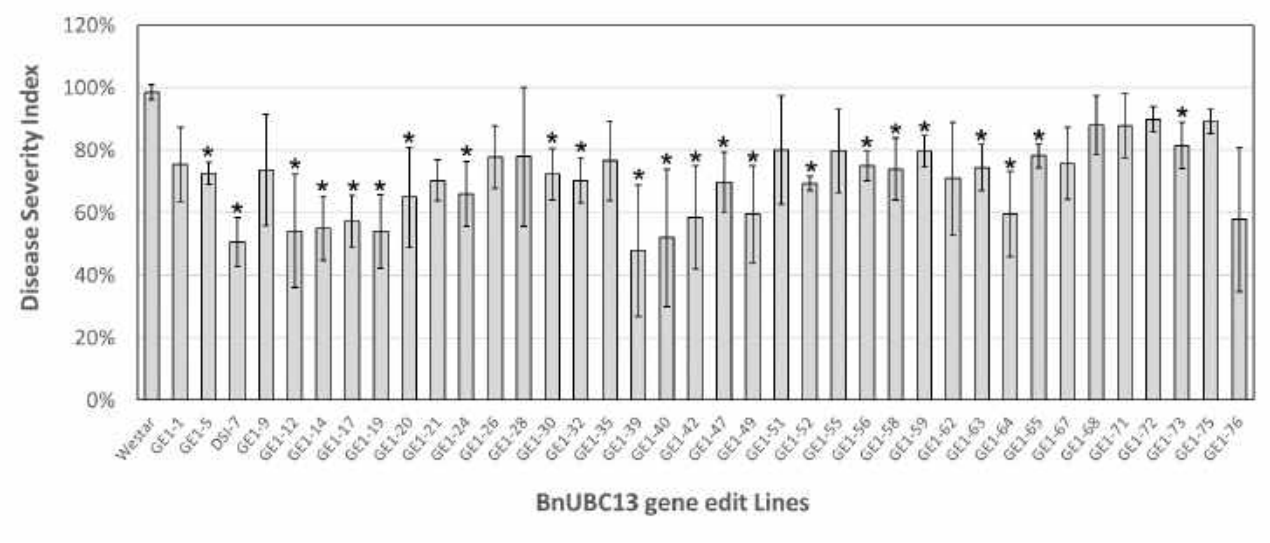

Figure 2.20 The disease severity index of clubroot in gene edited plants after soil inoculation with *P. brassicae* Pathotype 3H. **P*<0.01.

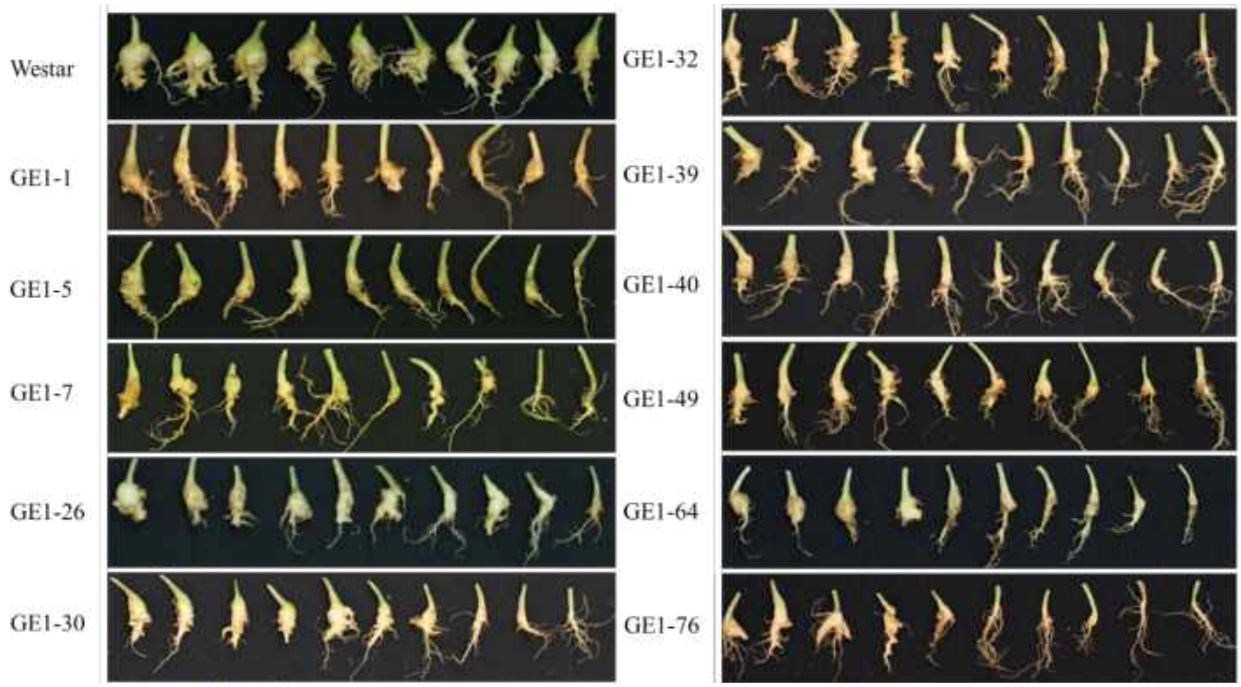

Figure 2.21 The root disease phenotype of canola plant at 28 dpi

To identify CRISPR/Cas9 edited mutation in each *BnUBC13* gene, gene specific primers around sgRNA target site were designed based on genomic DNA sequence of 12 *BnUBC13* genes (Table 2.3). Figure 2.22 shows that these primer sets can successfully disquingish each *BnUBC13* gene based on their PCR fragment size in agarose gel and were used to amplify targeting region.

Table 2.3 The information of gene specific primers targeting 12 *BnUBC13* genes.

Target gene ID	Amp. Length (bp)	Primer ID	Sequence (5'-3')	GC (%)	Tm (°C)
BnaA06g11360D	547	A6g113-gFP	TCGGTTCCTTTTTTTTTGGAG	38	48.5
		A6g113-gRP	TAAGGGACATTTAATGAACG	35	45.6
BnaA07g34450D	1388	A7g344-gFP	CGAGGAGCGCGTCAGATTCTATC	57	58.8
		A7g344-gRP	CTAATGTAATCAACTCATACG	33	46.5
BnaA08g23450D	1136	A8g234-gFP	TTGTTTCGCGTATCCGATC	47	48.9
		A8g234-gRP	GGAGAATAAGAGAGTGTCAACG	45	53
BnaAnng13030D	1277	Ang130-gFP	TTTCCCGATCTCTTTAAGTTGCC	43	53.5
		Ang130-gRP	GCTGCATATGTCCACATTGC	50	51.8
BnaC05g12900D	742	C5g129-gFP	ATCGATCAAAACGGATAGCAAGC	43	53.5
		C5g129-gRP	GAAAAACATGGCGGGTGATG	50	51.8
BnaC06g39290D	979	C6g392-gFP	GATTCCTGATTCTCATTTTTTGTC	33	50.6
		C6g392-gRP	CAGTCTGCGTAACACAACCAG	52	54.4
BnaC08g17090D	338	C8g170-gFP	CGATCTCGATTTCTCTCAGC	50	51.8
		C8g170-gRP	CACAACACTTGAAACCAAGTTAG	39	51.7
BnaC08g38130D	479	C8g381-gFP	ACGTAGCATCCGTTGCTAGC	55	53.8
		C8g381-gRP	CGTTAATACACAAGAATTAGTTC	30	48.1
BnaC06g20310D	603	C6g203-gFP	AAAGTGTTCTCTTGATCATCGG	41	51.1
		C6g203-gRP	CGAGATAAACATCTTGTAAACC	36	49.2
BnaC02g25260D	818	C2g252-gFP	AACTCTTATCGATCGAGCGAG	48	52.4
		C2g252-gRP	CCAATATCATTAAACACAGCCC	41	51.1
BnaA07g38410D	997	A7g384-gFP	CCCAAATCTATCTCATTTAGACG	39	51.7
		A7g384-gRP	CAAAATCATCAAAAGAGCCCG	43	50.5
BnaA02g19070D	878	A2g190-gFP	AGCGTGCGGATCTTCTCTCTC	57	56.3
		A2g190-gRP	GAATGGTGGTACATAGGTGAGG	50	54.8

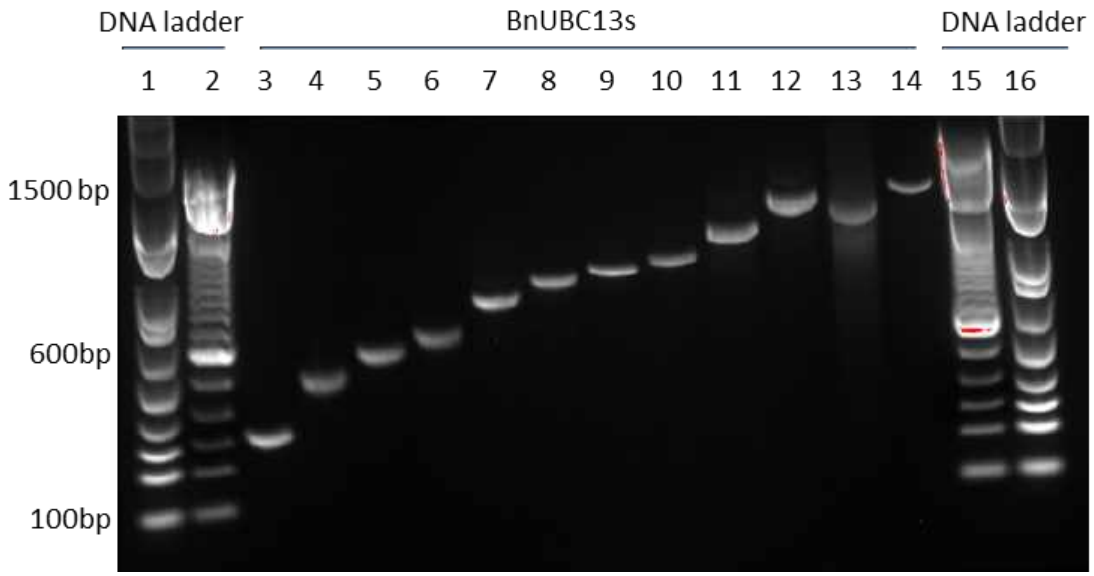

Figure 2.22 12 *BnUBC13* genes distinquished by gene-specific primers. Lanes 1 and 16: GeneRular DNA ladder mix; Lanes 2 and 15: 100-bp DNA ladder; Lane 3: BnaC08g17090D (338 bp), Lane 4: BnaC08g38130D (479 bp), Lane 5: BnaA06g11360D (547 bp), Lane 6: BnaC06g20310D (603 bp), Lane 7: BnaC05g12900D (742 bp), Lane 8: BnaC02g25260D (818 bp), Lane 9: BnaA02g19070D (878 bp), Lane 10: BnaC06g39290D (979 bp), Lane 11: BnaA08g23450D (1136 bp), Lane 12: BnaA07g38410D (1337 bp) Lane 13: BnaAnng13030D (1277 bp), Lane 14: BnaA07g34450D (1388 bp)

The first gene analyzed is *BnUBC13K* (BnaC06g20310D). The genomic DNA was extracted from T_0 plant leaves of 23 lines with significantly reduced disease severity (Figure 2.20) and 8 extra lines. The targeting region of each *BnUBC13* gene was amplified by gene-specific primers. The PCR fragments were purified and used for sequencing. Eighteen of 31 lines (58%) possessed mutations in close proximity to the protospacer adjacent motif (PAM) sequence. Six types of mutation variants were detected in these lines including single base insertions or deletions and base substitutions, but no large fragment deletions (Figure 2.23). The homozygous mutations were deceted in some lines that displayed clear single chromatograph peak at the mutation site, while the biallelic and monoallelic heterozygote mutations were identified as well based on the two overlapping chromatograph peaks at the mutation site (Figure 2.23). These mutations could cause seven types of amino acid (AA) alterations at the protein level, resulting in premature stop or AA substitutions (Table 2.4).

Then we analyzed the target sites at *BnUBC13H, I* and *L* loci, which have similar mutation types with *BnUBC13K.* The mutation analysis on *BnUBC13J* is still in progress. So far, two lines (GE1-5 and GE1-26) have been confirmed to have mutations on four *BnUBC13* genes. However, some mutations are heterozygote and need to be segregated into homozygote by the next generation. Meanwhile, the three other sgRNA constructs were pooled together and transformed into Agrobacterium. The canola transformation by these constructs is in progress.

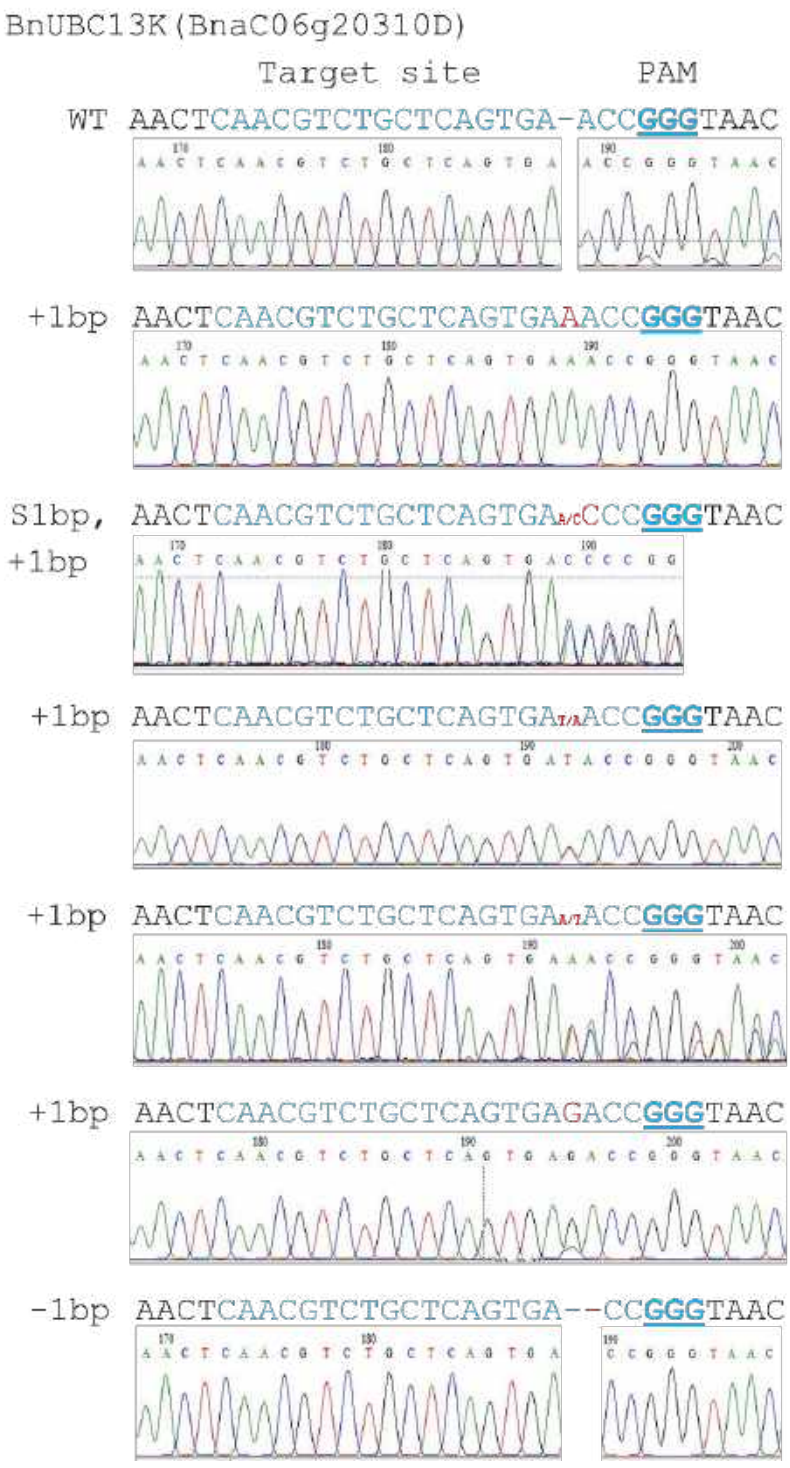

Figure 2.23 Different types of mutations at the *BnUBC13K* locus detected in GE plants. PAM, protospacer adjacent motif. The sgRNA targeting region is indicated in blue. The mutation sites are indicated in red. Corresponding sequencing chromatographs are shown below each sequence.

Table 2.4 The BnUbc13K amino acid changes caused by gene editing

Variant type	AA sequence in sgRNA region
Wild type	TQRLLSEPAPGISASPSEDN
Type 1	TQRLLSDPGSWYKCISI*
Type 2	TQRLLSETGSWYKCISI*
Type 3	TQRLLGDTAPGISASPSEDN
Type 4	TQRLLSDTGSWYKCISI*
Type 5	TQRLLSAPAPGISASPSEDN
Type 6	TQRLL-NQAPGISASPSEDN
Type 7	TQRLLSDRLLV*
Type 8	TQRLLSEPGSWYKCISI*

Amino acid sequence alignment of the target sites derived from WT and GE lines. Amino acids different from WT are indicated in red. * The premature stop codon.

2.4 Gene editing on *SWEET11* and *SWEET12* genes in canola

The clubroot pathogen relies on external sources of carbohydrates and the host manipulation to redirect carbohydrates from source leaves to underground roots to facilitate infection (Malinowski *et al.*, 2019). The pathogen-driven transportation of carbohydrates heavily relies on a group of genes called *SWEET* (Sugars Will Eventually be Exported Transporters), which play significant central roles in phloem loading and unloading sugars (Xue *et al.*, 2022). Arabidopsis *SWEET11* and *SWEET12* genes have been reported to contribute to clubroot disease development as susceptible factors (Li *et al.*, 2018, Walerowski *et al.*, 2018). However, their susceptible roles in *B. napus* have not been validated and confirmed yet.

Previous studies revealed that each of *SWEET* genes is expanded to five homologous genes in *B. napus* (Figure 2.24; Table 2.5) (Jian *et al.*, 2016). To create mutations in these genes, two sgRNA target sites for each gene group were designed and constructed into one CRISPR/Cas9 vector (Figure 2.25). Two transformation vectors were delivered into plants. Eventually, 55 and 70 regenerated plants were obtained for *SWEET11* and *SWEET12*, respectively. To narrow down candidate lines for the mutation analysis, a clubroot disease severity assessment was perfomed on T_1 plants of these lines (Figure 2.26). Compared to wild type control plants, the disease severity was dramatically reduced in gene edited lines: 11-25, 11-56, 11-57, 11-60, 12-2, 12-6 and 12-9. The mutation analysis on these lines is in progress.

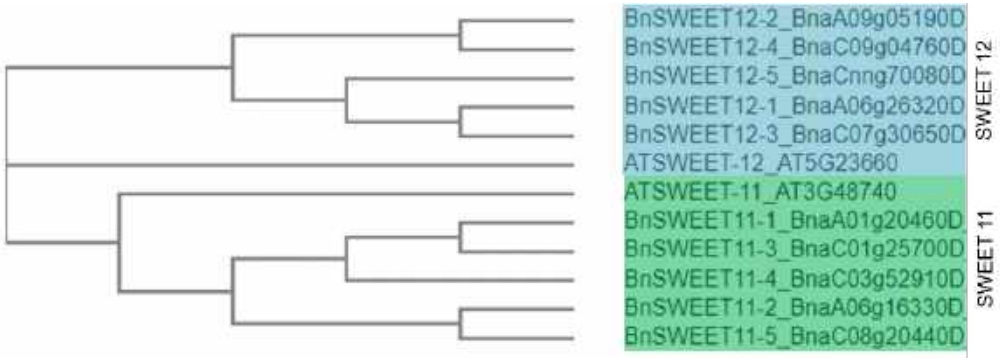

Figure 2.24 The phylogenetic analysis of *SWEET11* and *12* genes from *A. thaliana* and *B. napus*

Table 2.5 *Brassica napus SWEET11* and *12* genes (modified from Jian et al., 2016)

Isoforms	Transcript name	Arabidopsis Orthologs	Clade	gDNA size (bp)	exon	CDS size (nts)	Peptide residues
BnSWEET11-1	BnaA01g20460D	AT3G48740	III	3108	6	861	287
BnSWEET11-2	BnaA06g16330D	AT3G48740	III	2524	6	870	290
BnSWEET11-3	BnaC01g25700D	AT3G48740	III	2359	6	861	287
BnSWEET11-4	BnaC03g52910D	AT3G48740	III	2888	6	858	286
BnSWEET11-5	BnaC08g20440D	AT3G48740	III	2556	6	870	290
BnSWEET12-1	BnaA06g26320D	AT5G23660	III	2327	6	867	289
BnSWEET12-2	BnaA09g05190D	AT5G23660	III	2057	6	834	278
BnSWEET12-3	BnaC07g30650D	AT5G23660	III	1980	6	867	289
BnSWEET12-4	BnaC09g04760D	AT5G23660	III	1999	6	834	278
BnSWEET12-5	BnaCnng70080D	AT5G23660	III	1227	5	582	194

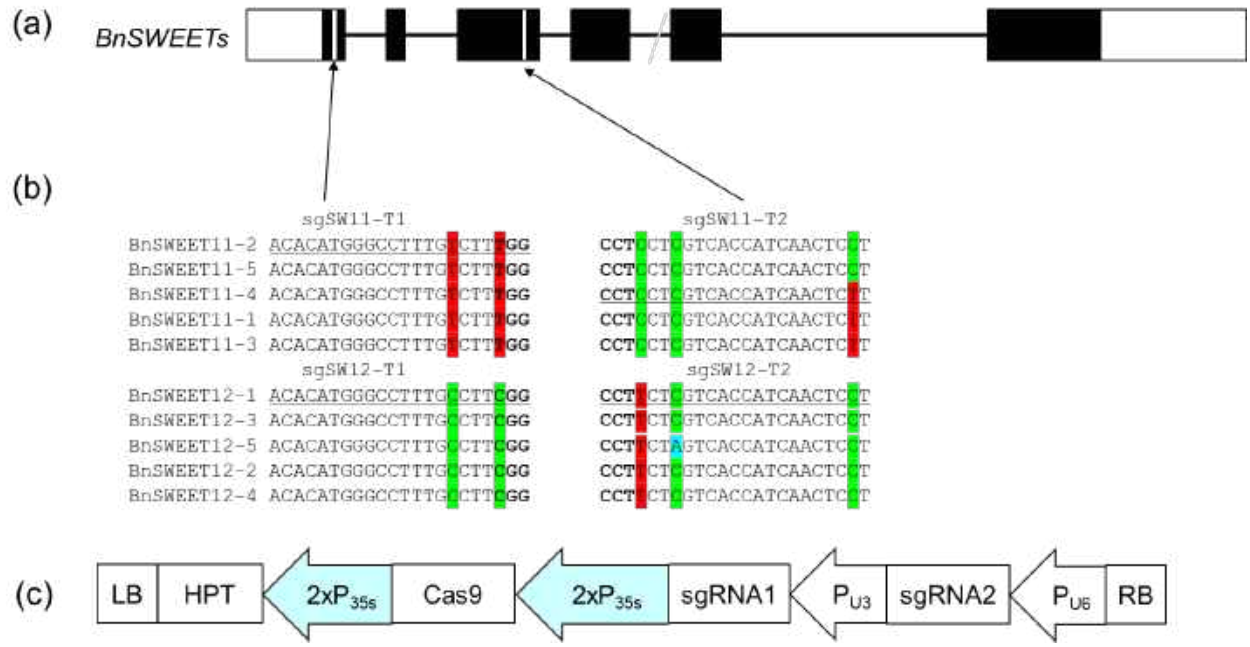

Figure 2.25 The *BnSWEET11/12* gene structure with target site sequences and the schematic Cas9/sgRNA vector. (a) Gene structure includes six exons (filled box) separated by introns (represented by solid lines). The vertical lines in the gene model indicates the target sites. (b) The sgRNA targeting sequences in each gene are shown and the PAM are highlighted in bold. SNPs between *SWEET11* and *SWEET12* are highlighted in red and green. (c) The construct of Cas9/sgRNA vector contains a hygromycin resistance cassette consisting of the hygromycin phosphotransferase (HPT) coding sequence driven by the cauliflower mosaic virus 35S promoter (P35S), a Cas9 expression cassette comprising the sequence encoding Cas9 driven by P35S, and sgRNA Sites 1 and 2 driven by U3 and U6 promoter, respectively.

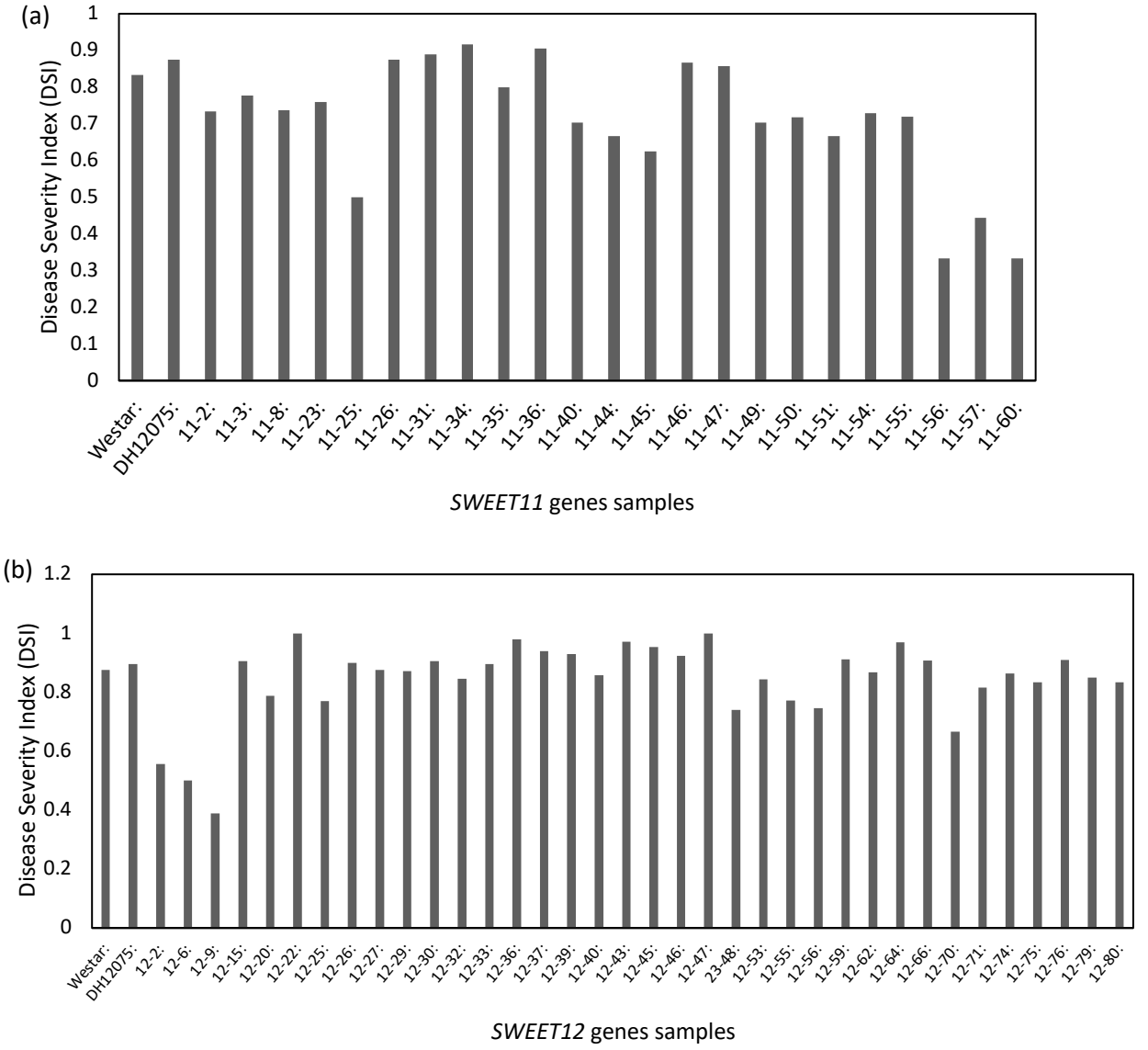

Figure 2.26 The disease severity index of clubroot in gene edited plants after soil inoculation with *P. brassicae* Pathotype 3H.

10. Conclusions and Recommendations: *Highlight significant conclusions based on the findings of this project, with emphasis on the project objectives specified above. Provide recommendations for the application and adoption of the project findings. (**Maximum of 500 words)***

In summary, this project successfully established an in-house CRISPR/Cas9 based genome editing platform that facilitates functional studies and trait characterization in *B. napus*. Beyond the clubroot resistance trait focused in this project, this platform can also be applied to any other agronomy trait development. This platform not only can be used to characterize and validate gene function, but also can help to modify deleterious alleles genetically linked to desirable traits via linkage drag, which cannot be fixed during conventional breeding process. An *S* gene based strategy to improve clubroot resistance has been developed and demonstrated in concept in this project, which is able to identify and characterize alleles that confer durable race-independent resistance against clubroot. With

increasing number of *S* genes characterized and introgressed into elite canola germplasms, the issue on resistance erosion by rapidly evolved pathogen is expected to be addressed in a near future. This study will expedite the breeding process and, consequently, reduce the investment costs to the canola industry in the breeding of new cultivars. Eventually, the knowledge, germplasm, molecular markers and CRISPR/Cas9 genome editing tools generated from this project will accelerate breeding cycles and benefit the Canadian canola industry.

11. Is there a need to conduct follow up research? *Detail any further research, development and/or communication needs arising from this project*.

Instead of editing single or a few genes at a time, current technology allows high througput genome-wide editing to edit a large number of genes simultaneously. Built on this project, we have developed a new project to scale up this platform and edit more *S* candidate genes. This new project has been granted by our industry parterners (SaskCanola and WGRF) and the NSERC Alliance program, in which a large-scale CRISPR/Cas9-mediated knockout mutant library targeting potential *S* genes will be established and validated genotypically and phenotypically. In addition, we will collaborate with scientists from NRC Nanotechnology Research Centre in Edmonton to advance the canola CRISPR/Cas9 genome editing platform by applying nanoparticle mediated delivery system to provide efficient transformation and transgene free plants.

12. Patents/ IP generated/ commercialized products: *List any products developed from this research.*

13. List technology transfer activities: *Include presentations to conferences, producer groups or articles published in science journals or other magazines*.

Invited presentations:

Wang, L., Wen. R., Peng, G. and **Xiao, W**. (2023) "Utilizing the susceptible gene and genome editing strategies to mitigate clubroot disease." *The Clubroot Workshop with Plant & Animal Genome Conference (PAG) 30*, January 13-18, San Diego, CA, USA

Wang, L., Wen. R., Peng, G. and **Xiao, W**. (2022) "Applying CRISPR/Cas9 genome editing to improve canola clubroot resistance." *Canola Week* 2022, December 6-8, Saskatoon, SK

Oral presentation:

Wang, L., Wen, R. and **Xiao, W**. (2018) "Translating basic knowledge to improve crop performance against biotic and abiotic stresses". *11th Canadian Plant Biotechnology Conference*, May 15-17, Saskatoon, SK

Poster presentations:

Wang, L., Wen, R., Kumasaruge, I., Tu, J., Peng, G. and Xiao, W. (2021) Improving clubroot resistance in canola through CRISPR/Cas9 based genome editing technology. *The Canadian Phytopathological Society, Tri-Society Virtual Conference*. July 5-9.

Wang, L., Wen, R. and Xiao, R. (2018) Plants employ two different types of programmed cell death in response to low temperature stress and pathogen invasion. *Fifth Joint Meeting of the Plant Pathology Society of Alberta & CPS-Saskatchewan Regional Meeting*, October 15-17, Lloydminster, SK

Publication:

Kumasaruge, I., Wen, R., Wang, L., Gao, P., Peng, G. and Xiao, W. (2023) Systematic characterization of *Brassica napus UBC13* genes involved in DNA-damage response and K63-linked polyubiquitination. *BMC Plant Biology*, 23: 24.

Magazine interview:

October 26, 2022 "Bringing CRISPR to canola - Gene editing for improved clubroot resistance – and more" *Top Crop Manager* https://www.topcropmanager.com/bringing-crispr-to-canola/

14. List any industry contributions or support received.

15. Acknowledgements. *Include actions taken to acknowledge support by the Ministry of Agriculture and the Canada-Saskatchewan Growing Forward 2 bilateral agreement (for projects approved during 2013-2017) or Canadian Agriculture Partnership (For projects approved beyond 2017).*

16. Appendices: *Include any additional materials supporting the previous sections, e.g. detailed data tables, maps, graphs, specifications, literature cited (Use a consistent reference style throughout).*

References:

Bartel, P.L. and Fields, S. (1995) Analyzing protein-protein interactions using two-hybrid system. *Methods Enzymol*, **254**, 241-263.

Broomfield, S., Chow, B.L. and Xiao, W. (1998) MMS2, encoding a ubiquitin-conjugating-enzyme-like protein, is a member of the yeast error-free postreplication repair pathway. *Proc Natl Acad Sci U S A*, **95**, 5678-5683.

Brusky, J., Zhu, Y. and Xiao, W. (2000) UBC13, a DNA-damage-inducible gene, is a member of the error-free postreplication repair pathway in Saccharomyces cerevisiae. *Current genetics*, **37**, 168-174.

Fan, L., Bi, T., Wang, L. and Xiao, W. (2020) DNA-damage tolerance through PCNA ubiquitination and sumoylation. *Biochem J*, **477**, 2655-2677.

Fields, S. and Song, O.-k. (1989) A novel genetic system to detect protein–protein interactions. *Nature*, **340**, 245-246.

Fukushima, T., Matsuzawa, S., Kress, C.L., Bruey, J.M., Krajewska, M., Lefebvre, S., Zapata, J.M., Ronai, Z. and Reed, J.C. (2007) Ubiquitin-conjugating enzyme Ubc13 is a critical component of TNF receptor-associated factor (TRAF)-mediated inflammatory responses. *Proc Natl Acad Sci U S A*, **104**, 6371-6376.

Garcia-Ruiz, H., Szurek, B. and Van den Ackerveken, G. (2021) Stop helping pathogens: engineering plant susceptibility genes for durable resistance. *Curr Opin Biotechnol*, **70**, 187-195.

Guo, K. and Li, L. (2009) Differential 12C-/13C-isotope dansylation labeling and fast liquid chromatography/mass spectrometry for absolute and relative quantification of the metabolome. *Anal Chem*, **81**, 3919-3932.

Hatakeyama, K., Suwabe, K., Tomita, R.N., Kato, T., Nunome, T., Fukuoka, H. and Matsumoto, S. (2013) Identification and characterization of Crr1a, a gene for resistance to clubroot disease (Plasmodiophora brassicae Woronin) in Brassica rapa L. *PLoS One*, **8**, e54745.

Hoege, C., Pfander, B., Moldovan, G.L., Pyrowolakis, G. and Jentsch, S. (2002) RAD6-dependent DNA repair is linked to modification of PCNA by ubiquitin and SUMO. *Nature*, **419**, 135-141.

Hofmann, R.M. and Pickart, C.M. (1999) Noncanonical MMS2-encoded ubiquitin-conjugating enzyme functions in assembly of novel polyubiquitin chains for DNA repair. *Cell*, **96**, 645-653.

Irani, S., Trost, B., Waldner, M., Nayidu, N., Tu, J., Kusalik, A.J., Todd, C.D., Wei, Y. and Bonham-Smith, P.C. (2018) Transcriptome analysis of response to Plasmodiophora brassicae infection in the Arabidopsis shoot and root. *BMC Genomics*, **19**, 23.

Jahn, L., Mucha, S., Bergmann, S., Horn, C., Staswick, P., Steffens, B., Siemens, J. and Ludwig-Müller, J. (2013) The Clubroot Pathogen (Plasmodiophora brassicae) Influences Auxin Signaling to Regulate Auxin Homeostasis in Arabidopsis. *Plants*, **2**, 726-749.

Jian, H., Lu, K., Yang, B., Wang, T., Zhang, L., Zhang, A., Wang, J., Liu, L., Qu, C. and Li, J. (2016) Genome-Wide Analysis and Expression Profiling of the SUC and SWEET Gene Families of Sucrose Transporters in Oilseed Rape (Brassica napus L.). *Frontiers in Plant Science*, **7**.

Letunic, I. and Bork, P. (2021) Interactive Tree Of Life (iTOL) v5: an online tool for phylogenetic tree display and annotation. *Nucleic Acids Research*, **49**, W293-W296.

Li, H., Li, X., Xuan, Y., Jiang, J., Wei, Y. and Piao, Z. (2018) Genome Wide Identification and Expression Profiling of SWEET Genes Family Reveals Its Role During Plasmodiophora brassicae-Induced Formation of Clubroot in Brassica rapa. *Front Plant Sci*, **9**, 207.

Li, W. and Schmidt, W. (2010) A lysine-63-linked ubiquitin chain-forming conjugase, UBC13, promotes the developmental responses to iron deficiency in Arabidopsis roots. *Plant J*, **62**, 330-343.

Ludwig-Müller, J., Prinsen, E., Rolfe, S.A. and Scholes, J.D. (2009) Metabolism and Plant Hormone Action During Clubroot Disease. *Journal of Plant Growth Regulation*, **28**, 229-244.

Ma, X., Zhang, Q., Zhu, Q., Liu, W., Chen, Y., Qiu, R., Wang, B., Yang, Z., Li, H., Lin, Y., Xie, Y., Shen, R., Chen, S., Wang, Z., Chen, Y., Guo, J., Chen, L., Zhao, X., Dong, Z. and Liu, Y.G. (2015) A Robust CRISPR/Cas9 System for Convenient, High-Efficiency Multiplex Genome Editing in Monocot and Dicot Plants. *Mol Plant*, **8**, 1274-1284.

Malinowski, R., Truman, W. and Blicharz, S. (2019) Genius Architect or Clever Thief—How Plasmodiophora brassicae Reprograms Host Development to Establish a Pathogen-Oriented Physiological Sink. *Molecular Plant-Microbe Interactions®*, **32**, 1259-1266.

Pastushok, L., Moraes, T.F., Ellison, M.J. and Xiao, W. (2005) A Single Mms2 "Key" Residue Insertion into a Ubc13 Pocket Determines the Interface Specificity of a Human Lys63 Ubiquitin Conjugation Complex*. *Journal of Biological Chemistry*, **280**, 17891-17900.

Rahman, H., Peng, G., Yu, F., Falk, K.C., Kulkarni, M. and Selvaraj, G. (2014) Genetics and breeding for clubroot resistance in Canadian spring canola (Brassica napus L.). *Canadian Journal of Plant Pathology*, **36**, 122-134.

Sander, J.D. and Joung, J.K. (2014) CRISPR-Cas systems for editing, regulating and targeting genomes. *Nat Biotechnol*, **32**, 347-355.

Scheben, A., Wolter, F., Batley, J., Puchta, H. and Edwards, D. (2017) Towards CRISPR/Cas crops - bringing together genomics and genome editing. *New Phytol*, **216**, 682-698.

Schuller, A., Kehr, J. and Ludwig-Müller, J. (2014) Laser microdissection coupled to transcriptional profiling of Arabidopsis roots inoculated by Plasmodiophora brassicae indicates a role for brassinosteroids in clubroot formation. *Plant Cell Physiol*, **55**, 392-411.

Siemens, J., Keller, I., Sarx, J., Kunz, S., Schuller, A., Nagel, W., Schmülling, T., Parniske, M. and Ludwig-Müller, J. (2006) Transcriptome analysis of Arabidopsis clubroots indicate a key role for cytokinins in disease development. *Mol Plant Microbe Interact*, **19**, 480-494.

van Schie, C.C. and Takken, F.L. (2014) Susceptibility genes 101: how to be a good host. *Annu Rev Phytopathol*, **52**, 551-581.

Wagner, G., Charton, S., Lariagon, C., Laperche, A., Lugan, R., Hopkins, J., Frendo, P., Bouchereau, A., Delourme, R., Gravot, A. and Manzanares-Dauleux, M.J. (2012) Metabotyping: a new approach to investigate rapeseed (Brassica napus L.) genetic diversity in the metabolic response to clubroot infection. *Mol Plant Microbe Interact*, **25**, 1478-1491.

Walerowski, P., Gündel, A., Yahaya, N., Truman, W., Sobczak, M., Olszak, M., Rolfe, S., Borisjuk, L. and Malinowski, R. (2018) Clubroot Disease Stimulates Early Steps of Phloem Differentiation and Recruits SWEET Sucrose Transporters within Developing Galls. *Plant Cell*, **30**, 3058-3073.

Wang, L., Wen, R., Wang, J., Xiang, D., Wang, Q., Zang, Y., Wang, Z., Huang, S., Li, X., Datla, R., Fobert, P.R., Wang, H., Wei, Y. and Xiao, W. (2019) Arabidopsis UBC13 differentially regulates two

programmed cell death pathways in responses to pathogen and low-temperature stress. *New Phytol*, **221**, 919-934.

Wang, Y., Tang, H., Debarry, J.D., Tan, X., Li, J., Wang, X., Lee, T.H., Jin, H., Marler, B., Guo, H., Kissinger, J.C. and Paterson, A.H. (2012) MCScanX: a toolkit for detection and evolutionary analysis of gene synteny and collinearity. *Nucleic Acids Res*, **40**, e49.

Wen, R., Newton, L., Li, G., Wang, H. and Xiao, W. (2006) Arabidopsis thaliana UBC13: implication of error-free DNA damage tolerance and Lys63-linked polyubiquitylation in plants. *Plant Mol Biol*, **61**, 241-253.

Wen, R., Torres-Acosta, J.A., Pastushok, L., Lai, X., Pelzer, L., Wang, H. and Xiao, W. (2008) Arabidopsis UEV1D promotes Lysine-63-linked polyubiquitination and is involved in DNA damage response. *Plant Cell*, **20**, 213-227.

Wen, R., Wang, S., Xiang, D., Venglat, P., Shi, X., Zang, Y., Datla, R., Xiao, W. and Wang, H. (2014) UBC13, an E2 enzyme for Lys63-linked ubiquitination, functions in root development by affecting auxin signaling and Aux/IAA protein stability. *Plant J*, **80**, 424-436.

Williamson, M.S., Game, J.C. and Fogel, S. (1985) Meiotic gene conversion mutants in Saccharomyces cerevisiae. I. Isolation and characterization of pms1-1 and pms1-2. *Genetics*, **110**, 609-646.

Wooff, J., Pastushok, L., Hanna, M., Fu, Y. and Xiao, W. (2004) The TRAF6 RING finger domain mediates physical interaction with Ubc13. *FEBS Lett*, **566**, 229-233.

Xiao, W., Chow, B.L., Fontanie, T., Ma, L., Bacchetti, S., Hryciw, T. and Broomfield, S. (1999) Genetic interactions between error-prone and error-free postreplication repair pathways in Saccharomyces cerevisiae. *Mutat Res*, **435**, 1-11.

Xiao, W. and Samson, L. (1993) In vivo evidence for endogenous DNA alkylation damage as a source of spontaneous mutation in eukaryotic cells. *Proc Natl Acad Sci U S A*, **90**, 2117-2121.

Xue, X., Wang, J., Shukla, D., Cheung, L.S. and Chen, L.Q. (2022) When SWEETs Turn Tweens: Updates and Perspectives. *Annu Rev Plant Biol*, **73**, 379-403.

Yang, K. and Xiao, W. (2022) Ubc13-UEV mediated K63-linked polyubiquitination in plants. *Journal of Experimental Botany*.

Yao, D., Arguez, M.A., He, P., Bent, A.F. and Song, J. (2021) Coordinated regulation of plant immunity by poly(ADP-ribosyl)ation and K63-linked ubiquitination. *Mol Plant*, **14**, 2088-2103.

Yin, K., Gao, C. and Qiu, J.L. (2017) Progress and prospects in plant genome editing. *Nat Plants*, **3**, 17107.

Yin, X.-J., Volk, S., Ljung, K., Mehlmer, N., Dolezal, K., Ditengou, F., Hanano, S., Davis, S.J., Schmelzer, E., Sandberg, G., Teige, M., Palme, K., Pickart, C. and Bachmair, A. (2007) Ubiquitin lysine 63 chain forming ligases regulate apical dominance in Arabidopsis. *The Plant cell*, **19**, 1898-1911.

Zaidi, S.S.-e.-A., Mukhtar, M.S. and Mansoor, S. (2018) Genome Editing: Targeting Susceptibility Genes for Plant Disease Resistance. *Trends in Biotechnology*, **36**, 898-906.

Zhang, Y. and Fernie, A.R. (2018) On the role of the tricarboxylic acid cycle in plant productivity. *Journal of integrative plant biology*, **60**, 1199-1216.

Zhou, Y., Wang, H., Gilmer, S., Whitwill, S., Keller, W. and Fowke, L.C. (2002) Control of petal and pollen development by the plant cyclin-dependent kinase inhibitor ICK1 in transgenic Brassica plants. *Planta*, **215**, 248-257.